MSTW2008 Parton Distributions - Uncertainties

Robert Thorne

May 29th, 2009

University College London

(In collaboration with A.D. Martin, W.J. Stirling and G. Watt)

MSTW08 – **New data included.**

NuTeV and CHORUS data on $F_2^{\nu,\bar{\nu}}(x,Q^2)$ and $F_3^{\nu,\bar{\nu}}(x,Q^2)$ replacing CCFR.

NuTeV and CCFR dimuon data included directly. Leads to a direct constraint on $s(x,Q^2)+\bar{s}(x,Q^2)$ and on $s(x,Q^2)-\bar{s}(x,Q^2)$. Affects other partons.

CDFII lepton asymmetry data in two different E_T bins – $25\mathrm{GeV} < E_T < 35\mathrm{GeV}$ and $35\mathrm{GeV} < E_T < 45\mathrm{GeV}$. D0II data for $E_T > 20\mathrm{GeV}$. First data sets only.

CDFII and D0II data on $d\,\sigma(Z)/d\,y$ for $0 < y < 3$.

HERA inclusive jet data (in DIS).

New CDFII and D0II high-p_T jet data.

Direct high-x data on $F_L(x,Q^2)$.

All published charm structure function data.

Would like averaged HERA structure function data.

MSTW08 – **Major changes in theory/approach.**

Implementation of updated heavy flavour VFNS, particularly at NNLO. Already use in MRST06 NNLO distributions, but not in official NLO sets. (Already used a general VFNS since 1998 but change in details.)

Inclusion of NNLO corrections (Anastasiou, Dixon, Melnikov, Petriello) Drell-Yan (W, Z and γ^*) data using Vrap and FEWZ.

Change in definition of α_S – same as QCDNUM, Pegasus. No Λ_{QCD} parameter.

Improved nuclear corrections, De Florian and Sassot obtained from NLO partons.

Implementation of fastNLO – fast perturbative QCD calculations Kluge, Rabbertz, Wobisch. Allows easy inclusion of new jet data from both Tevatron and HERA.

Change in means of obtaining uncertainties. Still diagonalise covariance matrix of parameters and use 20 (previously 15) orthogonal eigenvectors. Tolerance now determined differently.

Normalization uncertainties on data treated far more thoroughly.

Parton Uncertainties – Hessian Approach.

Hessian (Error Matrix) approach first used by H1 and ZEUS, and extended by CTEQ and used by MRST.

$$\chi^2 - \chi^2_{min} \equiv \Delta\chi^2 = \sum_{i,j} H_{ij}(a_i - a_i^{(0)})(a_j - a_j^{(0)})$$

The Hessian matrix H is related to the covariance matrix of the parameters by

$$C_{ij}(a) = \Delta\chi^2 (H^{-1})_{ij}.$$

We can then use the standard formula for linear error propagation.

$$(\Delta F)^2 = \Delta\chi^2 \sum_{i,j} \frac{\partial F}{\partial a_i}(H)^{-1}_{ij}\frac{\partial F}{\partial a_j},$$

This is now the standard approach.

However, somewhat inconvenient and problematic due to extreme variations in $\Delta\chi^2$ in different directions in parameter space.

Improved radically by finding and rescaling eigenvectors of H leading to diagonal form CTEQ

$$\Delta\chi^2 = \sum_i z_i^2$$

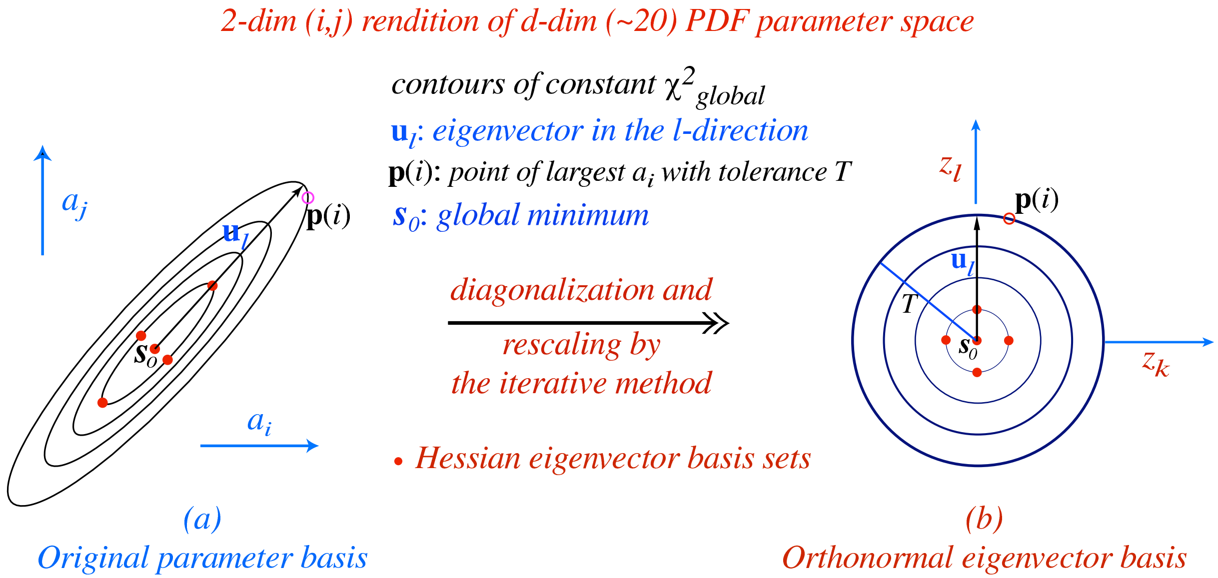

Implemented by CTEQ, then others. Uncertainty on physical quantity then given by

$$(\Delta F)^2 = \sum_i \left(F(S_i^{(+)}) - F(S_i^{(-)})\right)^2,$$

where $S_i^{(+)}$ and $S_i^{(-)}$ are PDF sets displaced along eigenvector direction by given $\Delta\chi^2$.

Traditionally $\Delta\chi^2 = 1$. Gives unbelievable uncertainties.

The inappropriateness of using $\Delta\chi^2 = 1$ when including a large number of sometimes conflicting data sets is shown by examining the best value of σ_W and its uncertainty using $\Delta\chi^2 = 1$ for individual data sets as obtained by CTEQ using Lagrange Multiplier technique.

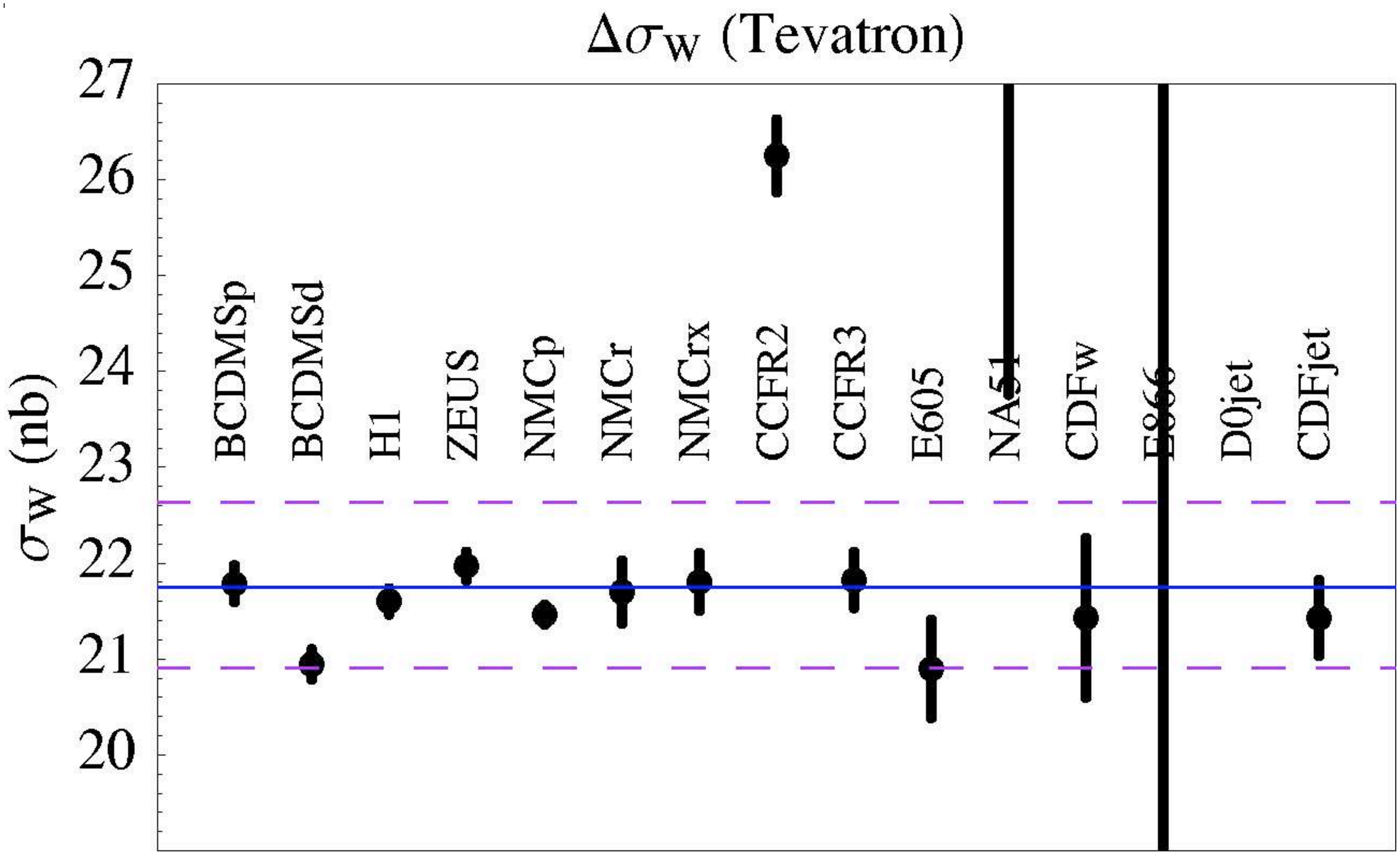

Previous reasoning, allow $\Delta\chi^2$ to take a value such that every data set remains roughly within its 90% confidence limit compared to the χ^2 at best global fit.

These limits shown for CTEQ6 eigenvector 4 as function of $T = \sqrt{\Delta\chi^2}$. Some sets somewhat outside 90% confidence limits for $T = 10$

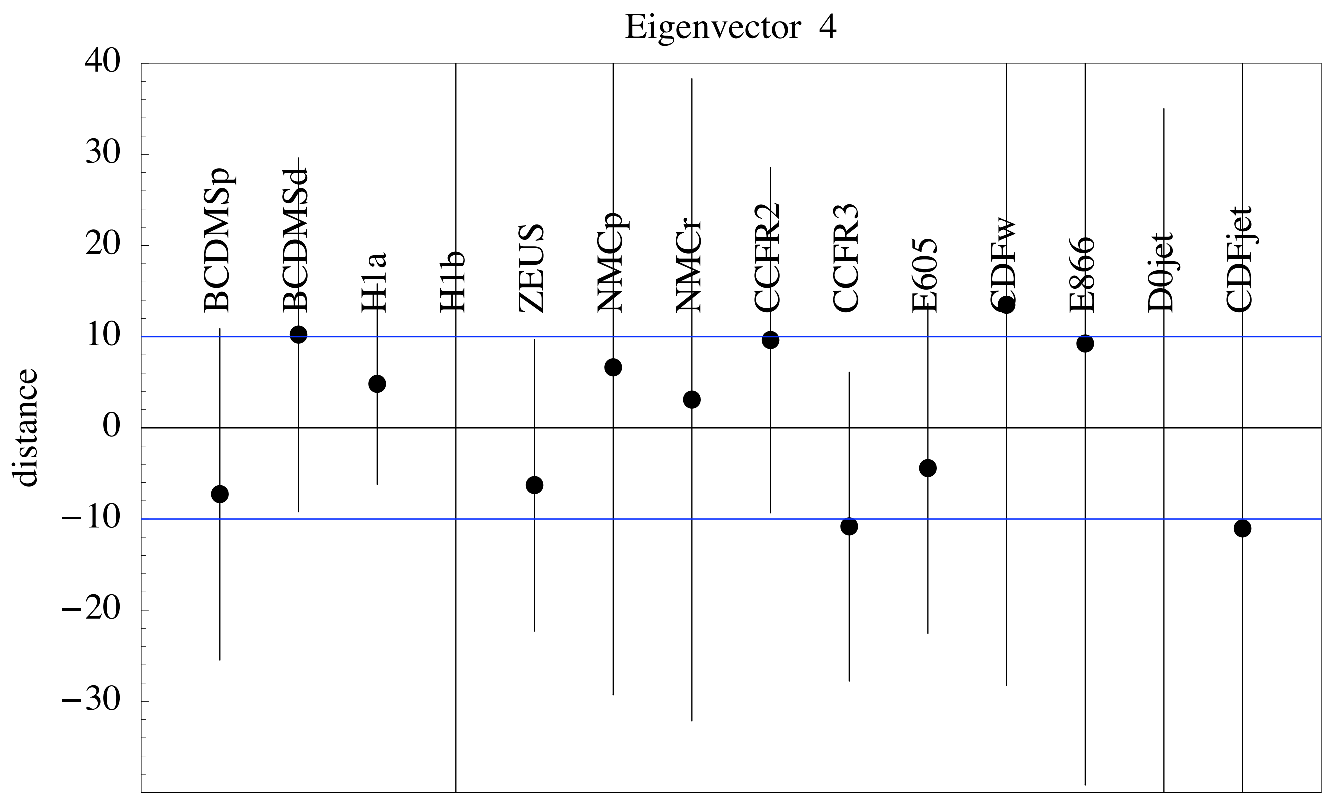

Using similar sort of reasoning MRST used $\Delta\chi^2 \sim 50$ for 90% confidence level on partons. Still same basic idea but more sophisticated.

Explained below (Watt DIS08)

- Define 90% C.L. region for each data set n (with N_n data points) as

$$\chi_n^2 < \left(\frac{\chi_{n,0}^2}{\xi_{50}}\right) \xi_{90}$$

- ξ_{90} is the 90th percentile of the χ^2-distribution with N_n d.o.f., i.e.

$$\int_0^{\xi_{90}} \mathrm{d}\chi^2 \, f(\chi^2; N_n) = 0.90,$$

  where the probability density function is

$$f(z; N) = \frac{z^{N/2-1} \, \mathrm{e}^{-z/2}}{2^{N/2} \, \Gamma(N/2)}.$$

- $\xi_{50} \simeq N_n$ is the most probable value of the χ^2-distribution.
- $\chi_{n,0}^2$ for data set n is evaluated at the **global** minimum.
- **Rescale** by a factor $\chi_{n,0}^2/\xi_{50}$ since this often deviates from 1.
- Similarly for the 68% C.L. region.

For eigenvector 13, for example, the change in χ^2 for the most sensitive data sets is shown.

For each determine the point in $\Delta\chi^2_{\rm global}$ at which the appropriate confidence level limit is reached in each direction.

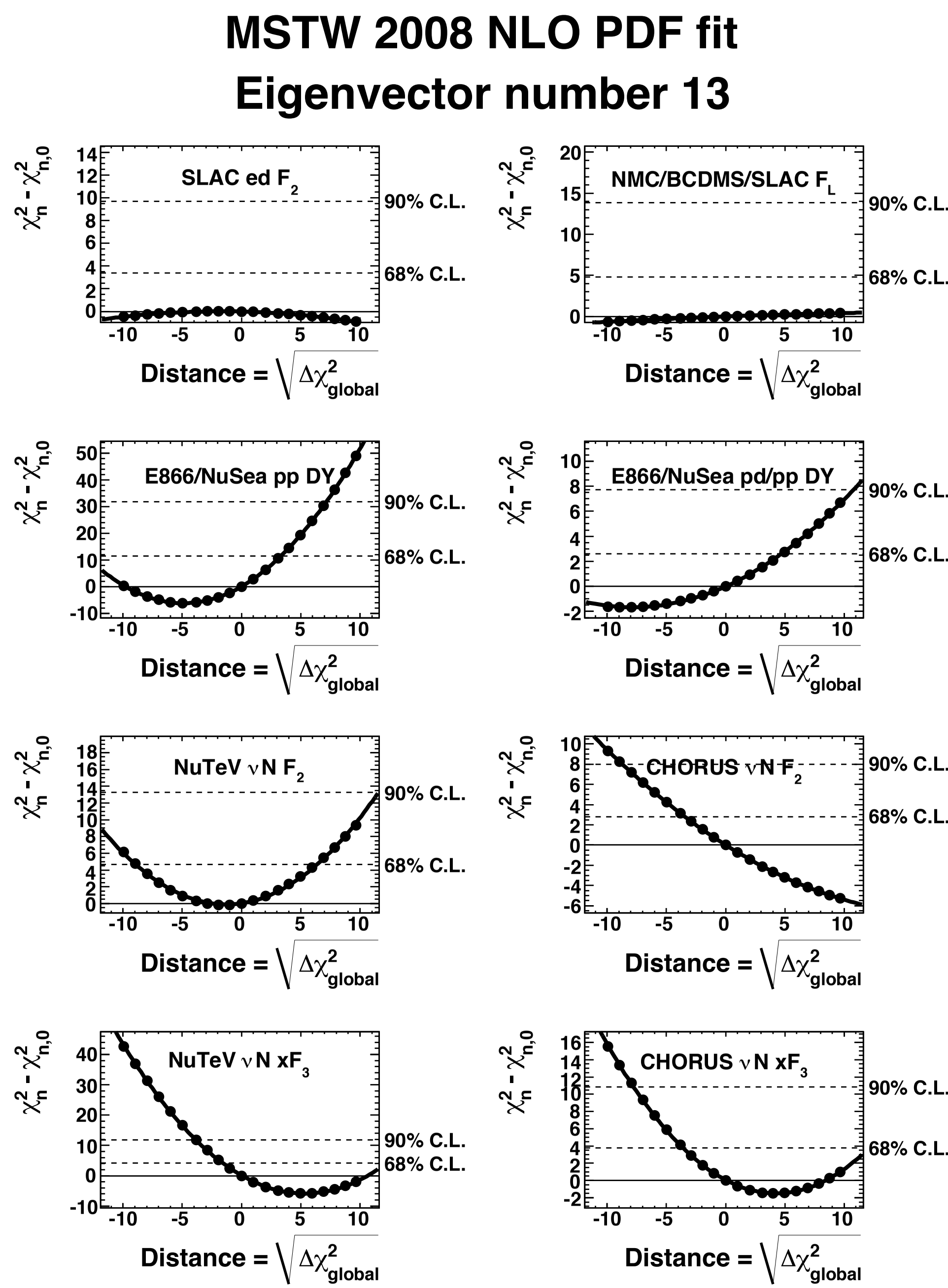

Plot this for all data sets for a given eigenvector.

Eigenvector 13 constrained in one direction by E866 Drell-Yan data and in the other direction by NuTeV $F_3^p(x, Q^2)$ data . In this case the best fits for the two sets are highly inconsistent. $\Delta\chi^2 = 100$ well outside 90% confidence level for each.

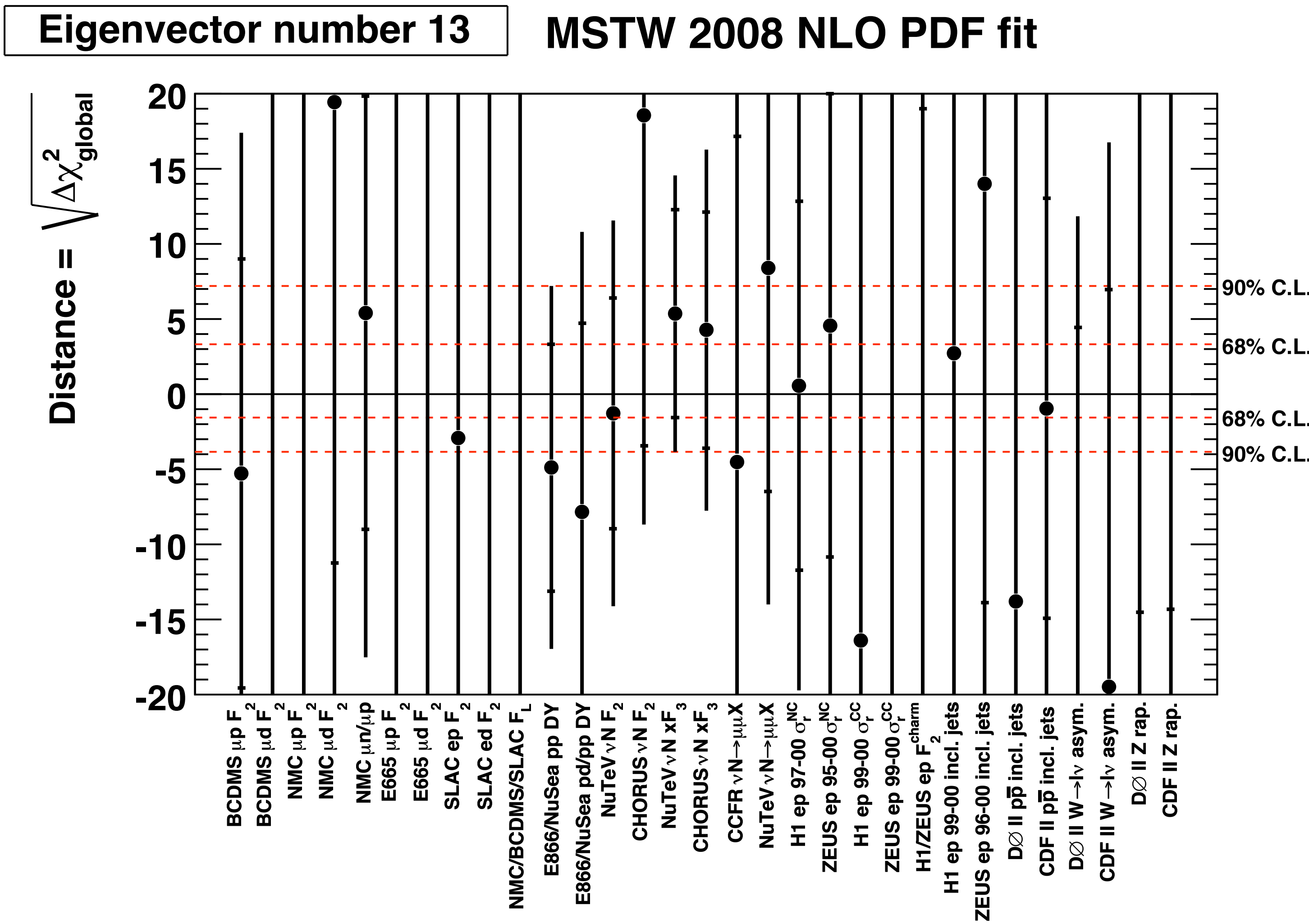

This eigenvector contributes most to the high-x sea quark uncertainty, but also a variety of other quarks.

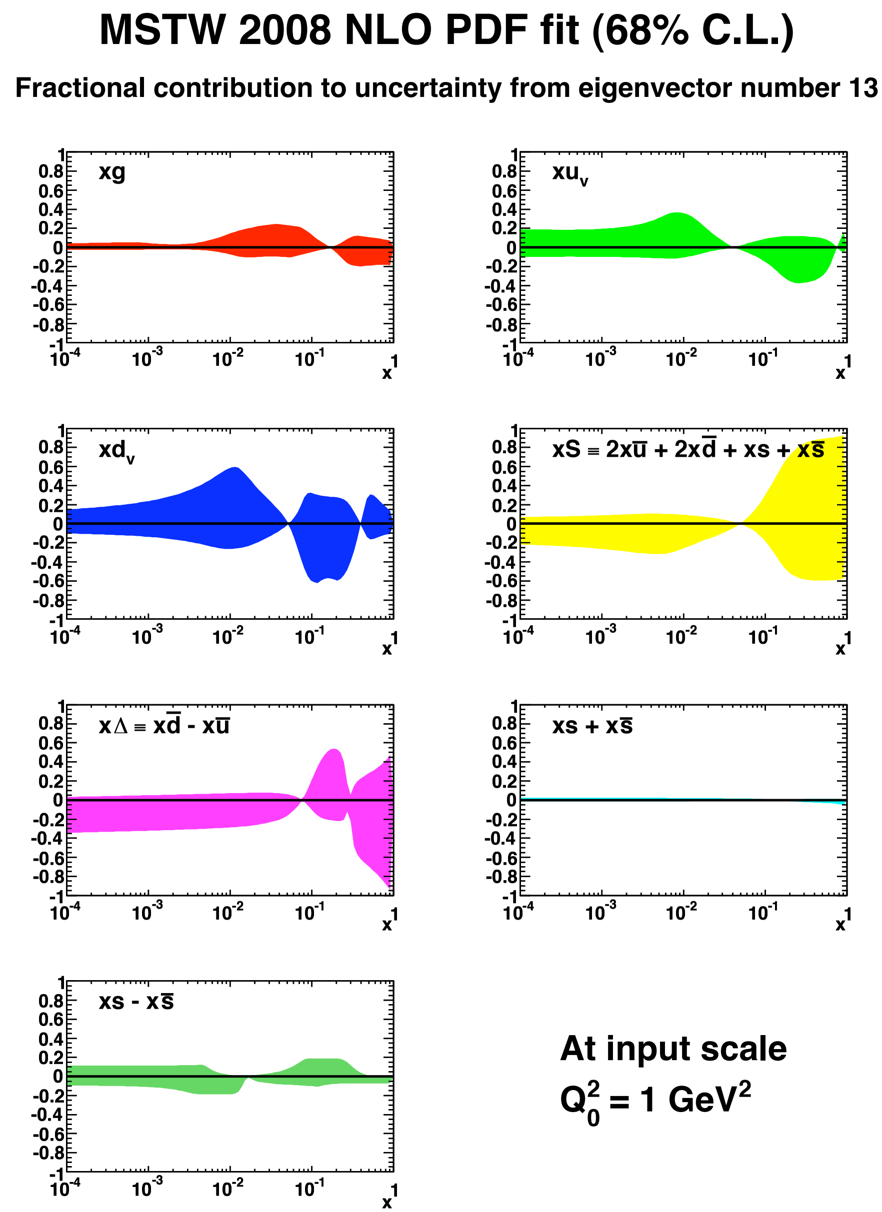

As a simpler example, eigenvector 9 constrained most by H1 and ZEUS data on $F_2^p(x, Q^2)$. 90% confidence limit determining by ZEUS in *up* direction and H1 in *down* direction. Both $\Delta\chi^2 \approx 50$.

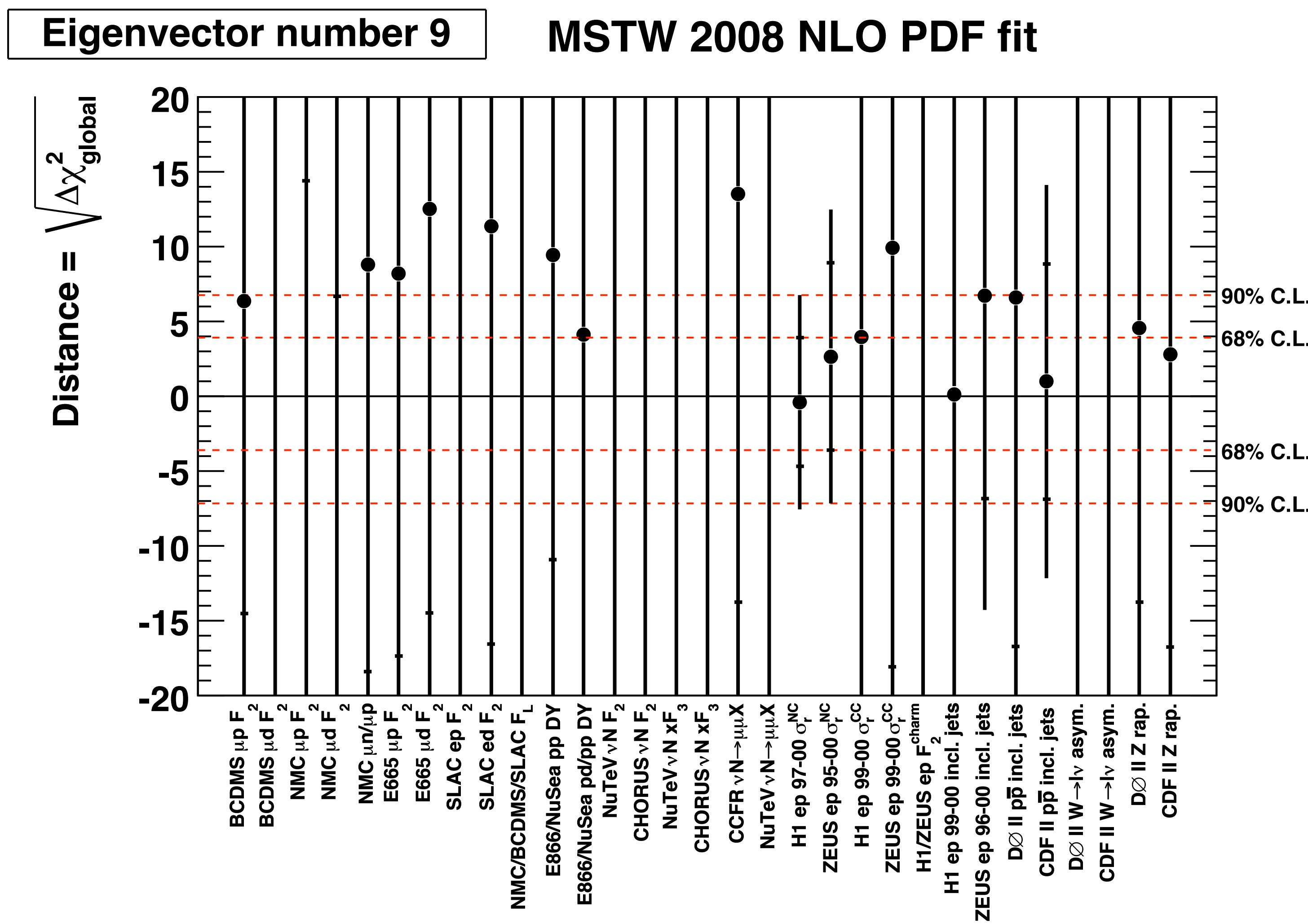

Not surprising this eigenvector contributes most to the gluon uncertainty.

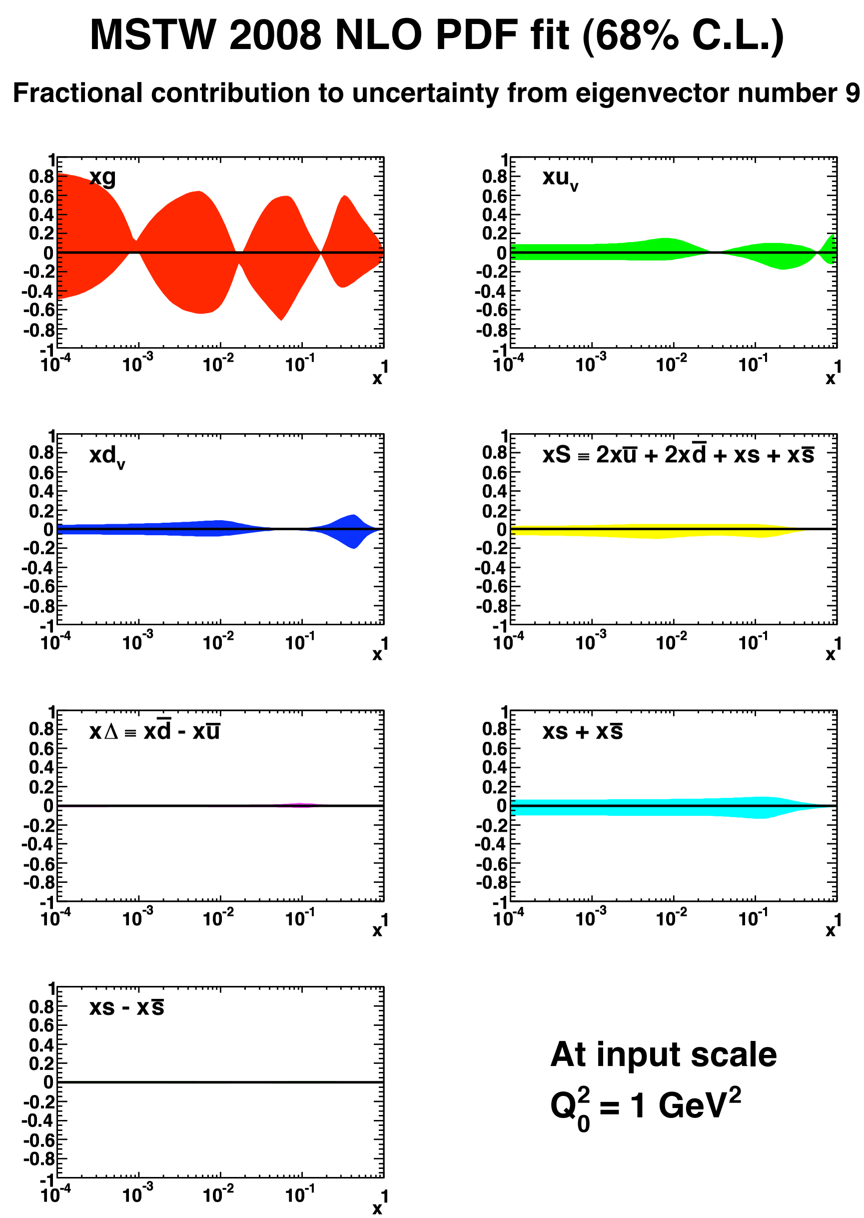

Approach repeated for all 20 eigenvectors to determine uncertainty on each. On average $\Delta\chi^2 = 40$ for 90% and $\Delta\chi^2 = 15$ for $1-\sigma$, but large variations, and asymmetries.

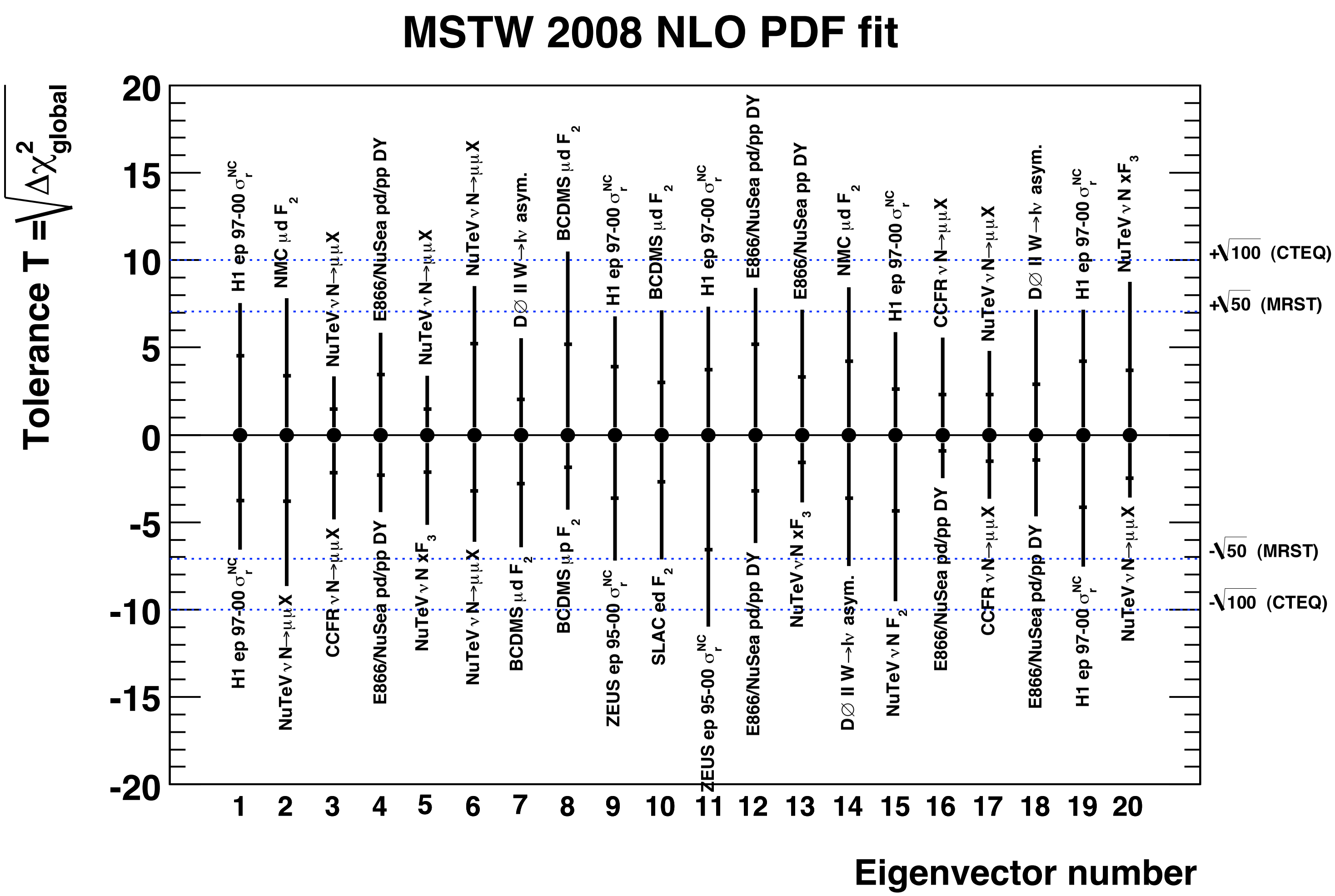

Normalisation Uncertainties

Previously the normalization of each data set was determined by the best fit – and then fixed.

Technical difficulties in including this feature in uncertainties.

Now implement procedure of allowing normalisations of all sets to vary in best fit and scan over eigenvectors, with penalty term for each set

$$\chi^2_{\mathcal{N}} = \left(\frac{1-\mathcal{N}}{\sigma^{\mathcal{N}}}\right)^4$$

Quartic penalty avoids very large deviations. Still shift down at LO (fit failure) and slightly at NLO.

Rescale errors with normalization to avoid bias (D'Agostini).

Data set	$\sigma_n^{\mathcal{N}}$	LO	NLO	NNLO
BCDMS μp F_2 [32]	3%	0.9667	0.9644	0.9678
BCDMS μd F_2 [102]	3%	0.9667	0.9644	0.9678
NMC μp F_2 [33]	2%	1.0083	0.9982	0.9999
NMC μd F_2 [33]	2%	1.0083	0.9982	0.9999
NMC $\mu n/\mu p$ [103]	—	1	1	1
E665 μp F_2 [104]	1.85%	1.0146	1.0052	1.0024
E665 μd F_2 [104]	1.85%	1.0146	1.0052	1.0024
SLAC ep F_2 [105, 106]	1.9%	1.0227	1.0125	1.0078
SLAC ed F_2 [105, 106]	1.9%	1.0227	1.0125	1.0078
NMC/BCDMS/SLAC F_L [32–34]	—	1	1	1
E866/NuSea pp DY [107]	6.5%	1.0629	1.0086	1.0868
E866/NuSea pd/pp DY [108]	—	1	1	1
NuTeV νN F_2 [37]	2.1%	0.9987	0.9997	0.9992
CHORUS νN F_2 [38]	2.1%	0.9987	0.9997	0.9992
NuTeV νN xF_3 [37]	2.1%	0.9987	0.9997	0.9992
CHORUS νN xF_3 [38]	2.1%	0.9987	0.9997	0.9992
CCFR $\nu N \to \mu\mu X$ [39]	2.1%	0.9987	0.9997	0.9992
NuTeV $\nu N \to \mu\mu X$ [39]	2.1%	0.9987	0.9997	0.9992
H1 MB 99 e^+p NC [31]	1.3%	0.9861	1.0098	1.0090
H1 MB 97 e^+p NC [109]	1.5%	0.9863	0.9921	0.9953
H1 low Q^2 96–97 e^+p NC [109]	1.7%	1.0029	1.0095	1.0172
H1 high Q^2 98–99 e^-p NC [110]	1.8%	0.9782	0.9851	0.9860
H1 high Q^2 99–00 e^+p NC [35]	1.5%	0.9762	0.9834	0.9842
ZEUS SVX 95 e^+p NC [111]	1.5%	0.9944	0.9948	1.0004
ZEUS 96–97 e^+p NC [112]	2%	0.9735	0.9811	0.9871
ZEUS 98–99 e^-p NC [113]	1.8%	0.9771	0.9855	0.9862
ZEUS 99–00 e^+p NC [114]	2.5%	0.9656	0.9761	0.9762
H1 99–00 e^+p CC [35]	1.5%	0.9762	0.9834	0.9842
ZEUS 99–00 e^+p CC [36]	2.5%	0.9656	0.9761	0.9762
H1/ZEUS ep $F_2^{\rm charm}$ [41–47]	—	1	1	1
H1 99–00 e^+p incl. jets [59]	1.5%	0.9762	0.9834	—
ZEUS 96–97 e^+p incl. jets [57]	2%	0.9735	0.9811	—
ZEUS 98–00 $e^{\pm}p$ incl. jets [58]	2.5%	0.9656	0.9761	—
DØ II $p\bar{p}$ incl. jets [56]	6.1%	0.9353	1.0596	1.0759
CDF II $p\bar{p}$ incl. jets [54]	5.8%	0.8779	0.9646	0.9900
CDF II $W \to \ell\nu$ asym. [48]	—	1	1	1
DØ II $W \to \ell\nu$ asym. [49]	—	1	1	1
DØ II Z rap. [53]	—	1	1	1
CDF II Z rap. [52]	5.8%	0.8779	0.9646	0.9900

Different groups all use different approaches.

Alekhin (Phys.Rev.D63:094022,2001) and older H1 (Eur.Phys.J.C30:1-32,2003) rescale uncertainties and quadratic penalty - textbook approach.

CTEQ (Phys.Rev.D65:014012,2002; Stump, PHYSTAT, 2003) allow normalisations to vary in best fit using quadratic penalty, but not when determining uncertainties. (No rescaling of errors, no apparent bias.)

Older ZEUS (Phys.Rev.D67:012007,2003) use the *Offset method* – fit normalisation in best fit and vary like other correlated errors when determining uncertainties.

More recent H1, ZEUS combination fits fit data to each other (quadratic penalty). Normalisations float towards each other and final uncertainty reduced.

NNPDF (Nucl.Phys.B809:1-63,2009) generate replica data sets by variations due to normalisation uncertainty. Covariance matrix for error function rescales other errors, but no explicit normalisation uncertainty – N_c number of correlated errors, bar represents rescaled error.

$$\overline{\mathrm{cov}}^{(k)}{}_{pq} = \left(\sum_{l=1}^{N_c} \overline{\sigma}^{(k)}{}_{p,l} \overline{\sigma}^{(k)}{}_{q,l} + \delta_{pq} \left(\overline{\sigma}^{(k)}{}_{p,s} \right)^2 \right) F_{I,p} F_{J,q}$$

Each data set spread around central value rather than floating. Larger uncertainty.

Comparison of full uncertainty and that from not normalization uncertainties (except in best fit).

Normalization uncertainty $\sim 1 - 1.5\%$, for all partons.

Difficult to account for in tolerance for eigenvectors – some very sensitive (size of quarks) others insensitive ($\bar{u} - \bar{d}$ determined from ratios).

During the scans variations in normalisation nearly always $\leq$ normalisation errors.

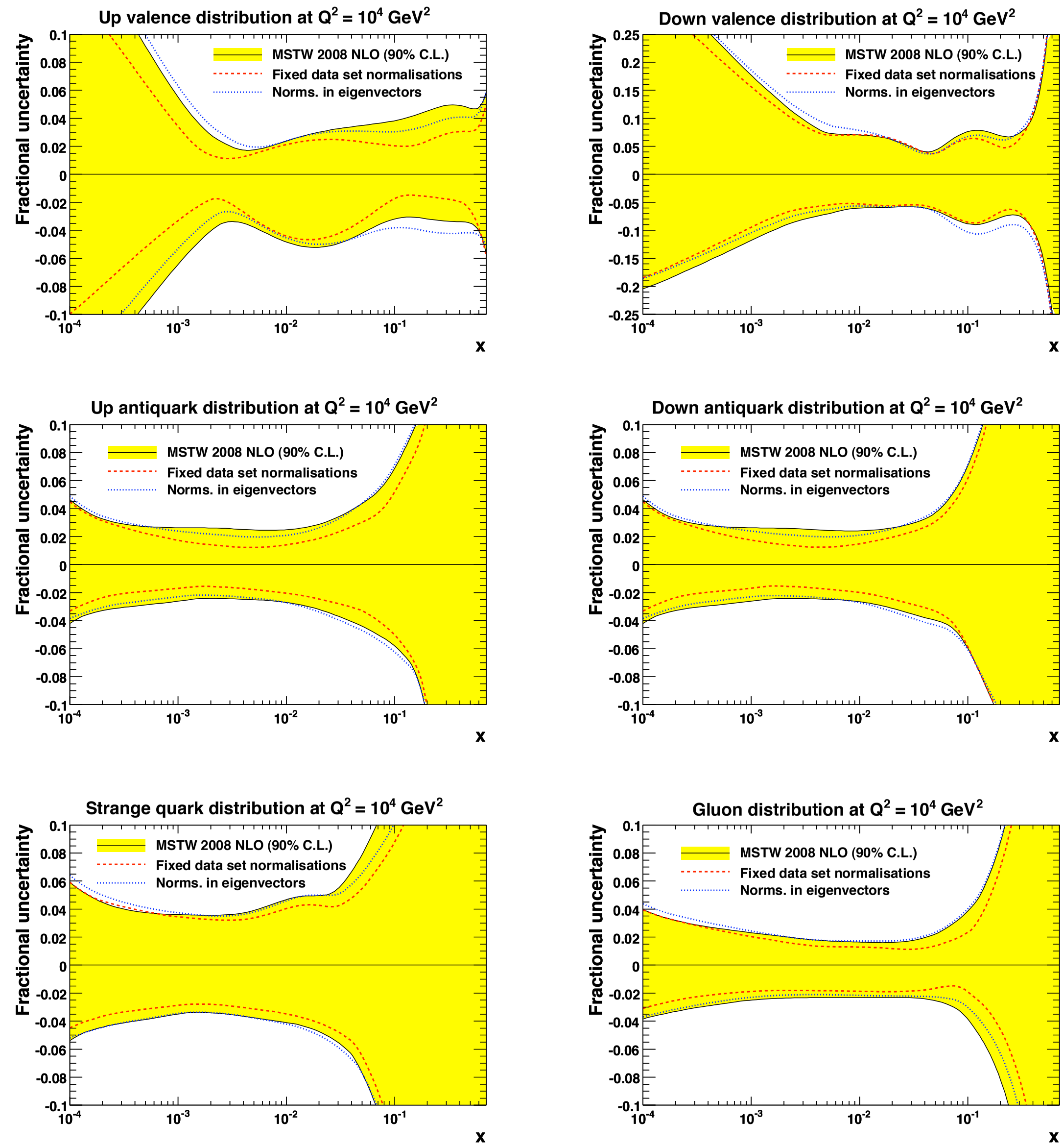

(blue) line, alternative (*equivalent*) approach (more efficient - less useful).

In practice should give a conservative estimation of uncertainties.

Can investigate by repeating HERA-LHC Workshop exercise of obtaining PDFs by fitting to DIS data with conservative cuts only.

Comparison of normal and benchmark sets shown.

Latter have greater uncertainty. Compatibility using *dynamical tolerance* uncertainty approach, but not using $\Delta\chi^2 = 1$.

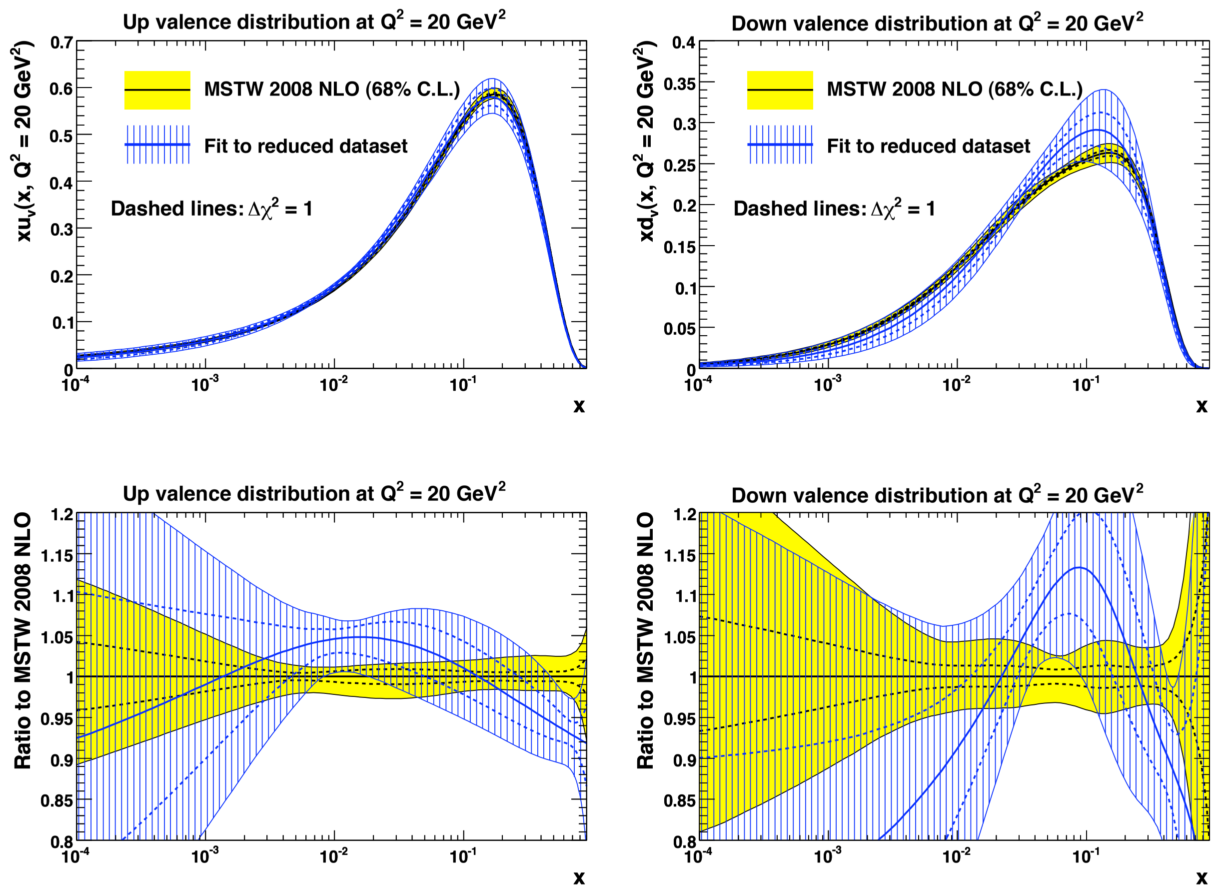

Still lack of compatibility some places, e.g high-x gluon.

Even though one data set constrains each eigenvector limit, doesn't mean others do not contribute.

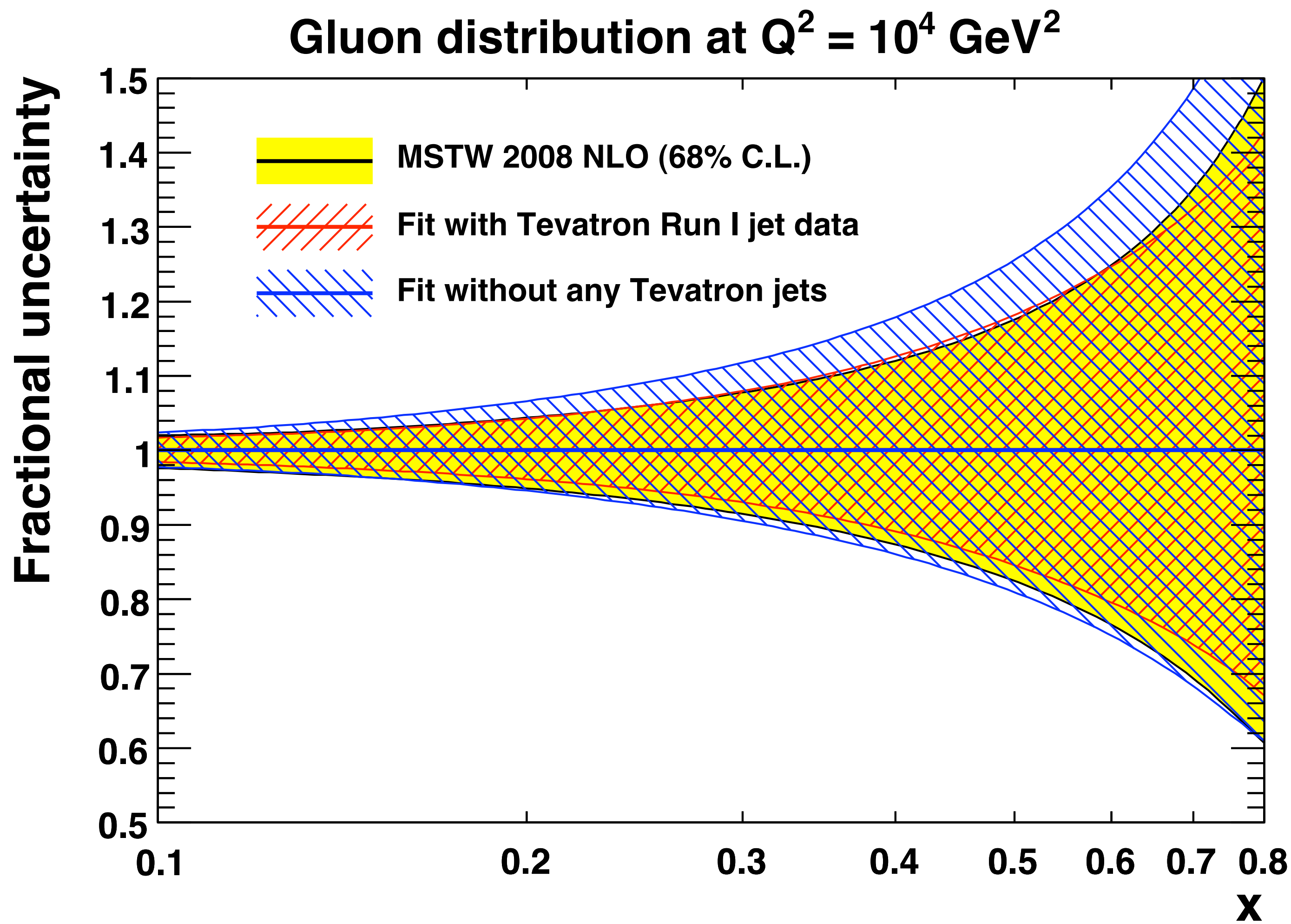

More on this topic in second talk.

Note that different parameterisations lead to very different types of uncertainty, particularly on small x gluon.

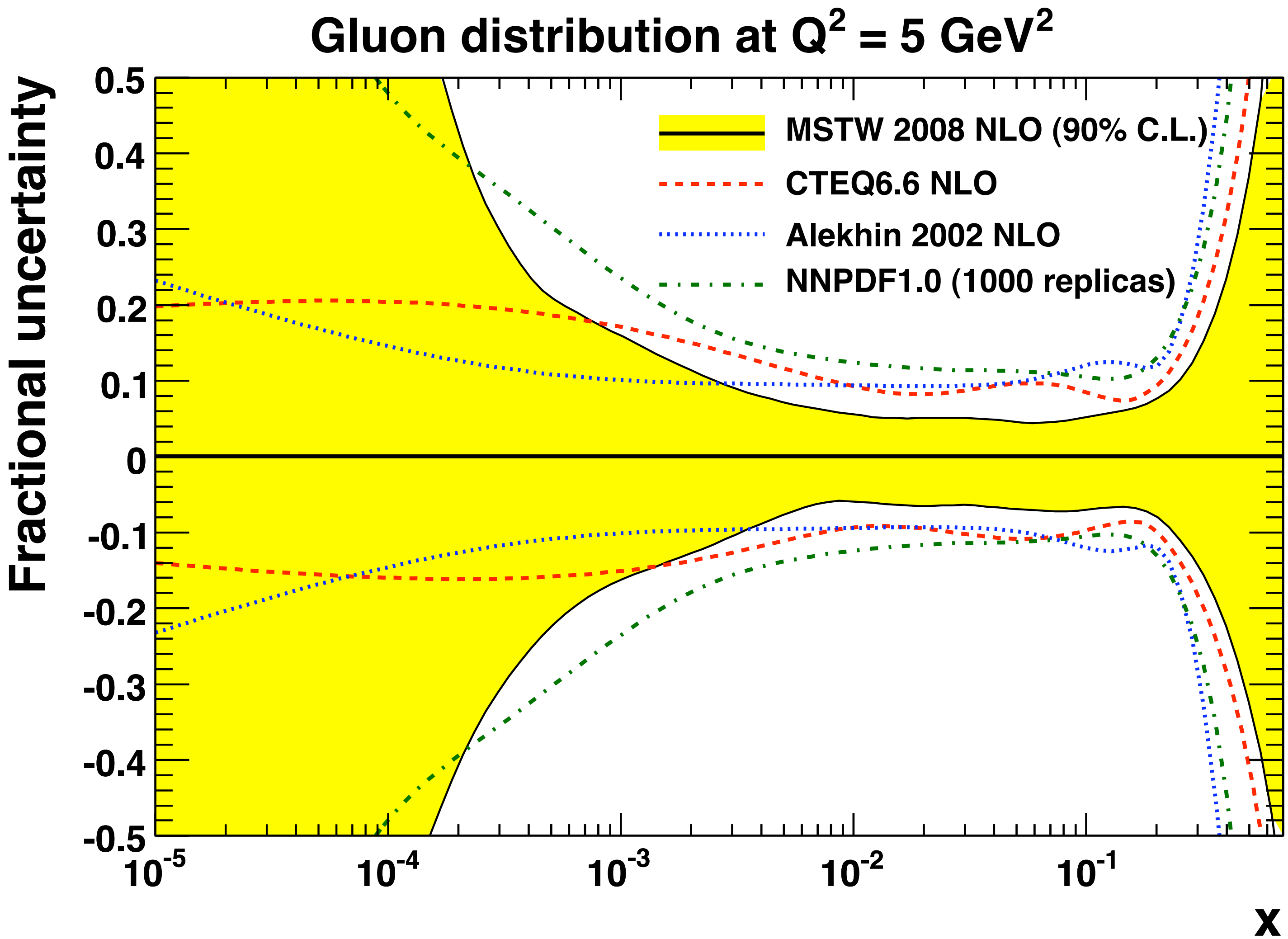

Overall $d_V(x, Q^2)$ now chooses a different type of shape.

Mainly changed by new $Tevatron$ W-asymmetry data and new neutrino structure function data.

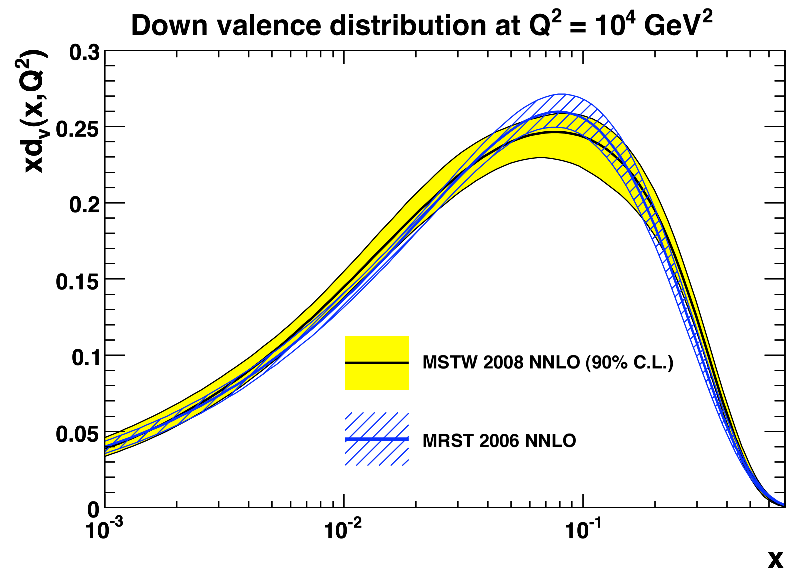

Uncertainty growing more quickly as $x \to 0$ and $x \to 1$ than before due to better parameterisation in determining uncertainty eigenvectors.

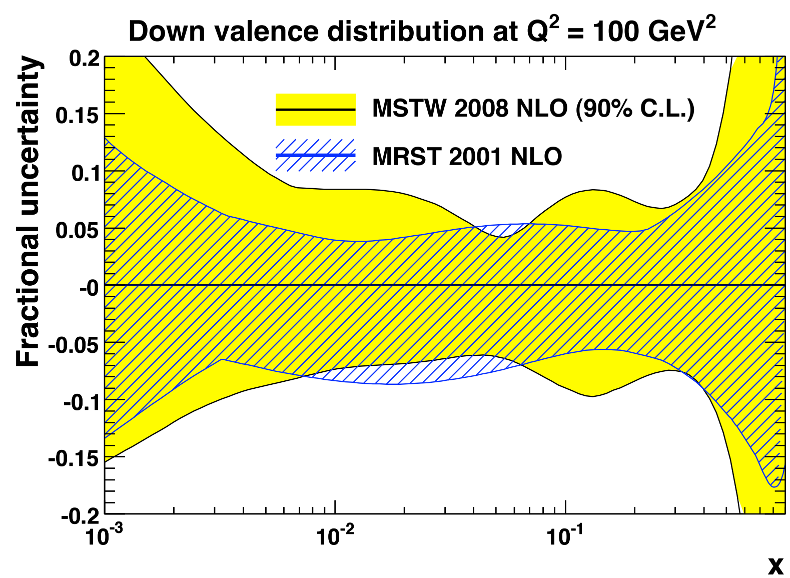

Direct fit to $s, \bar{s}$ from dimuon data leads to significant uncertainty increase compared to assumption of fixed fraction of sea.

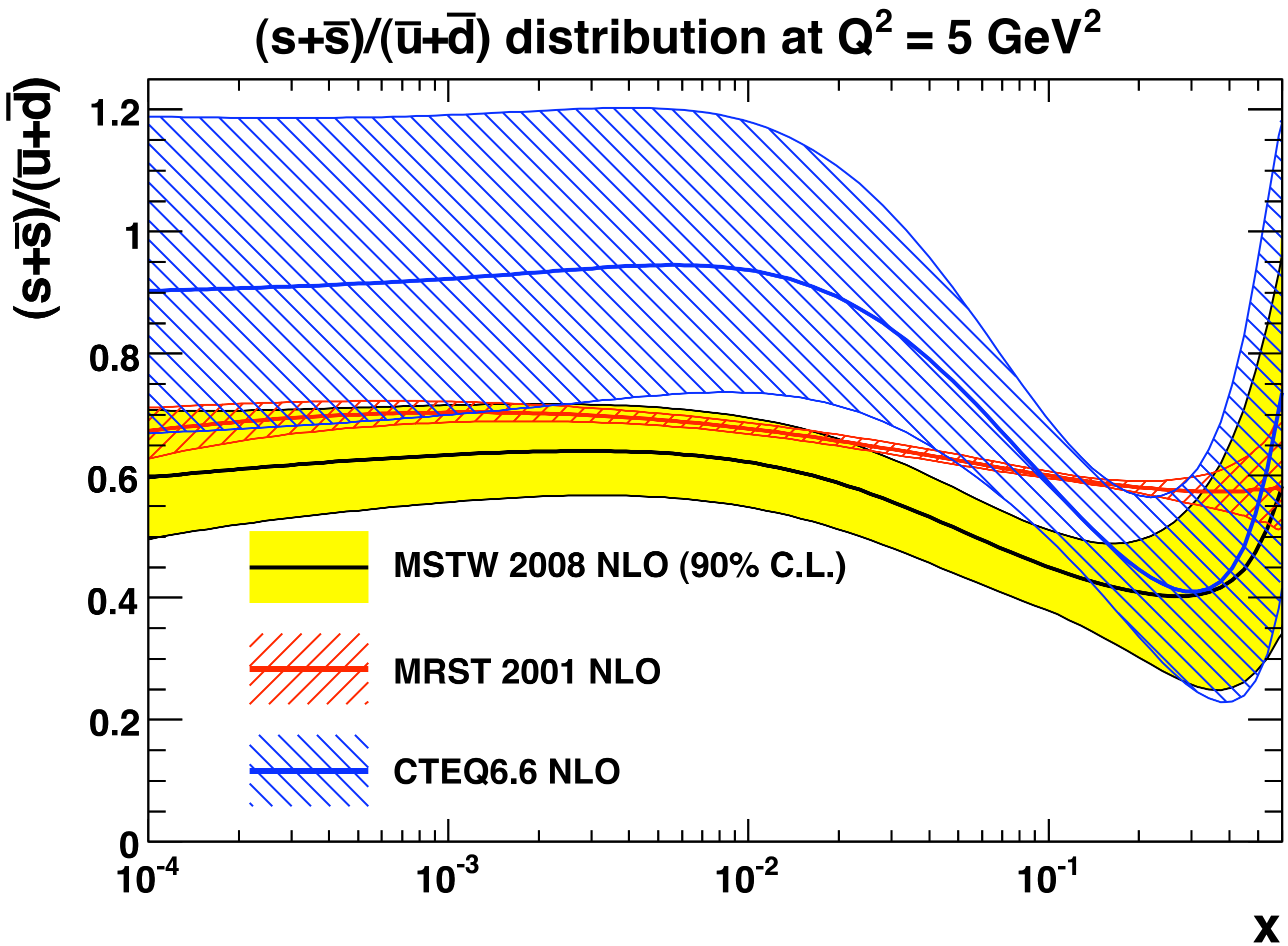

Significant difference to CTEQ fitting to same data. At small x assume shape of input sea quarks is the same (consistent with mass suppression) whereas CTEQ have different parameterisation.

Comparison to MRST2006 PDFs.

Generally larger uncertainties from normalization uncertainties and more flexible parameterisations. Tolerance for eigenvectors generally smaller.

Change in shapes of gluon due to new Tevatron jet data, in strange from fitting dimuon data and in down from Tevatron vector boson production and neutrino data.

Other changes partly due to lower $\alpha_S(M_Z^2)$, e.g. at NNLO goes from $0.119 \rightarrow 0.117$.

Uncertainties due to α_S variation also studied (not previously accounted for by anyone in uncertainty sets).

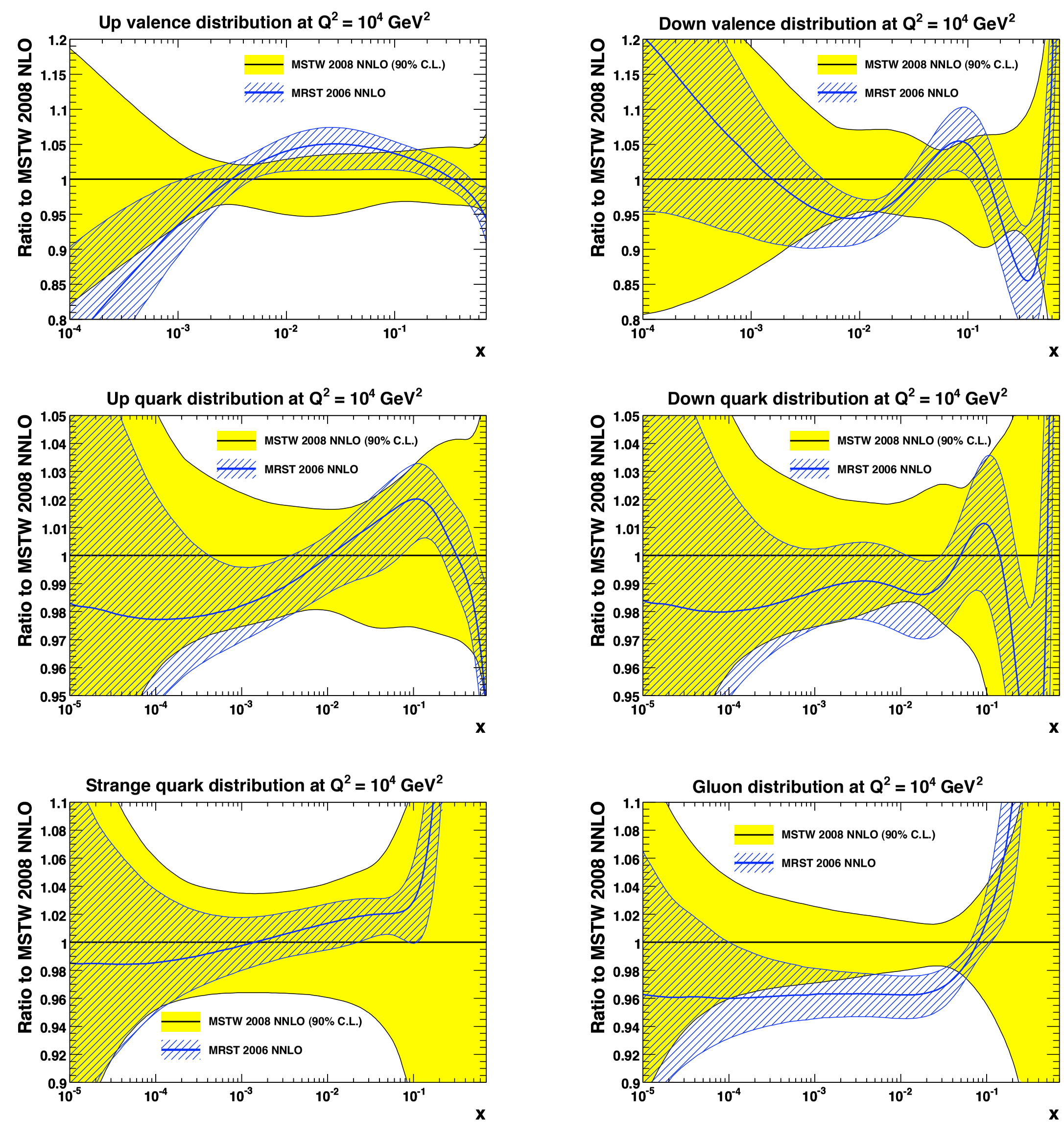

Comparison to CTEQ6.6 at NLO.

CTEQ strange now larger at small-x.

CTEQ gluon larger at high-x (run I jets) and small-x (input parameterization). Feeds into quark shape.

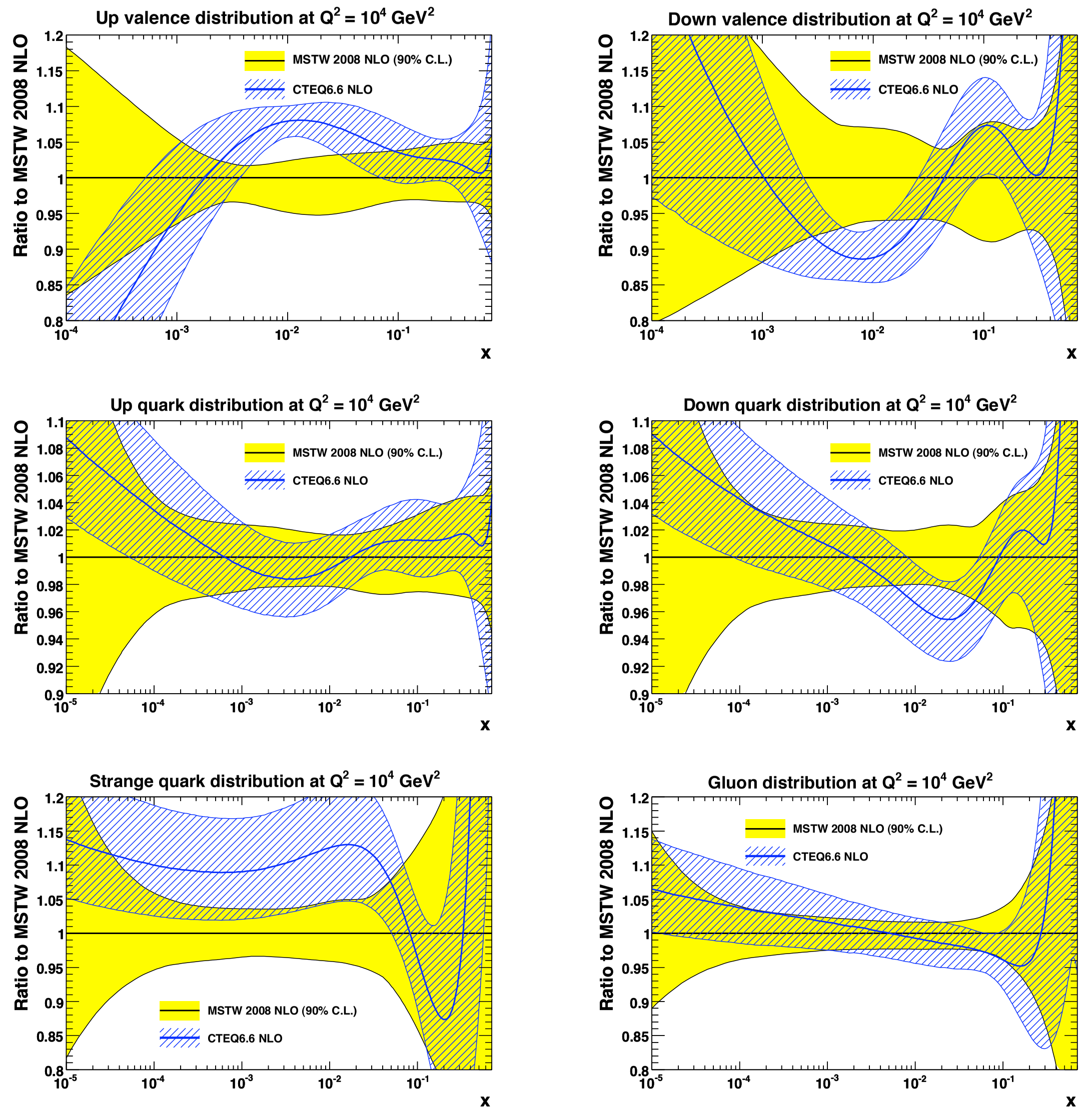

Comparison of uncertainties to NLO Neural Network PDF set.

Often comparable despite input flexibility in NNPDF.

Remember they use only DIS data.

Extra constraints from Tevatron W,Z and high-p_T jet data, Drell-Yan data *etc.*

Particularly important for quark flavour decomposition and impacts on gluon.

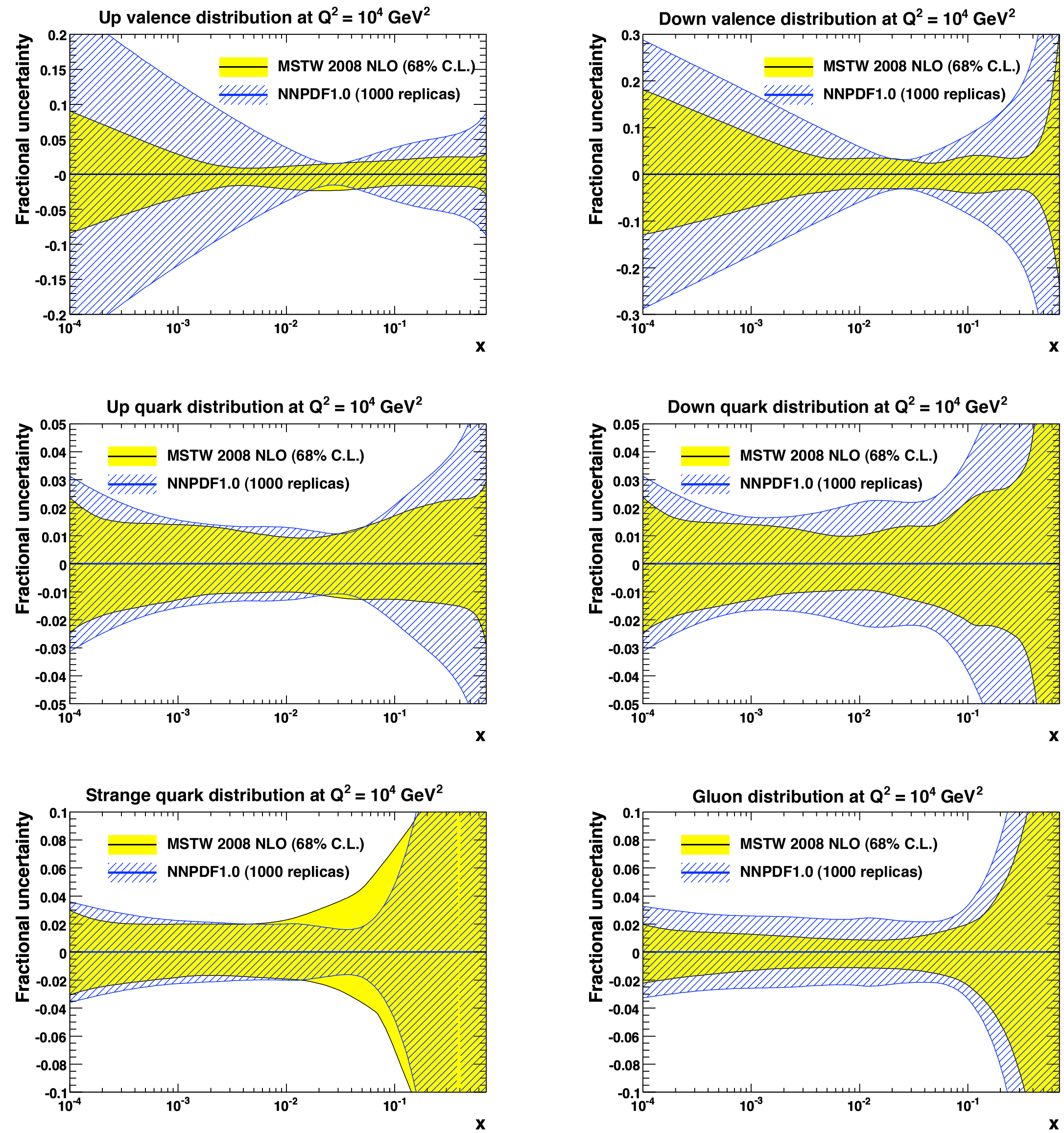

Kinematics at the LHC

Overall – new kinematic regime.

High scale and small-x parton distributions are vital for understanding processes at the LHC.

LHCb in particular probes regions of intrinsic (experimental) uncertainty

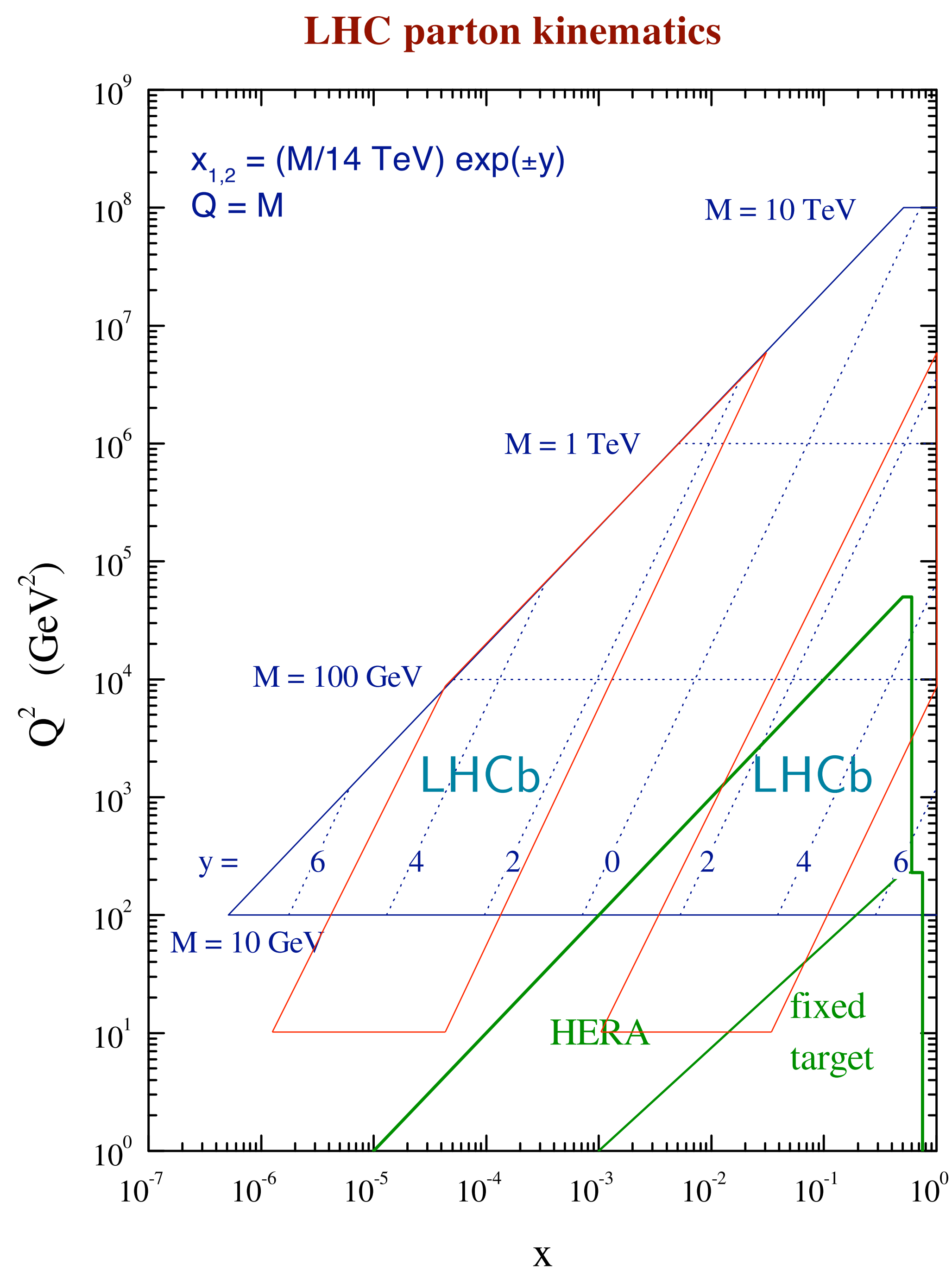

Parton Luminosity Uncertainties

Uncertainties on parton luminosities, i.e. of fundamental rates for creation processes, are optimum for standard model particle production.

Start to worsen at highest masses where sensitive to large-x PDFs.

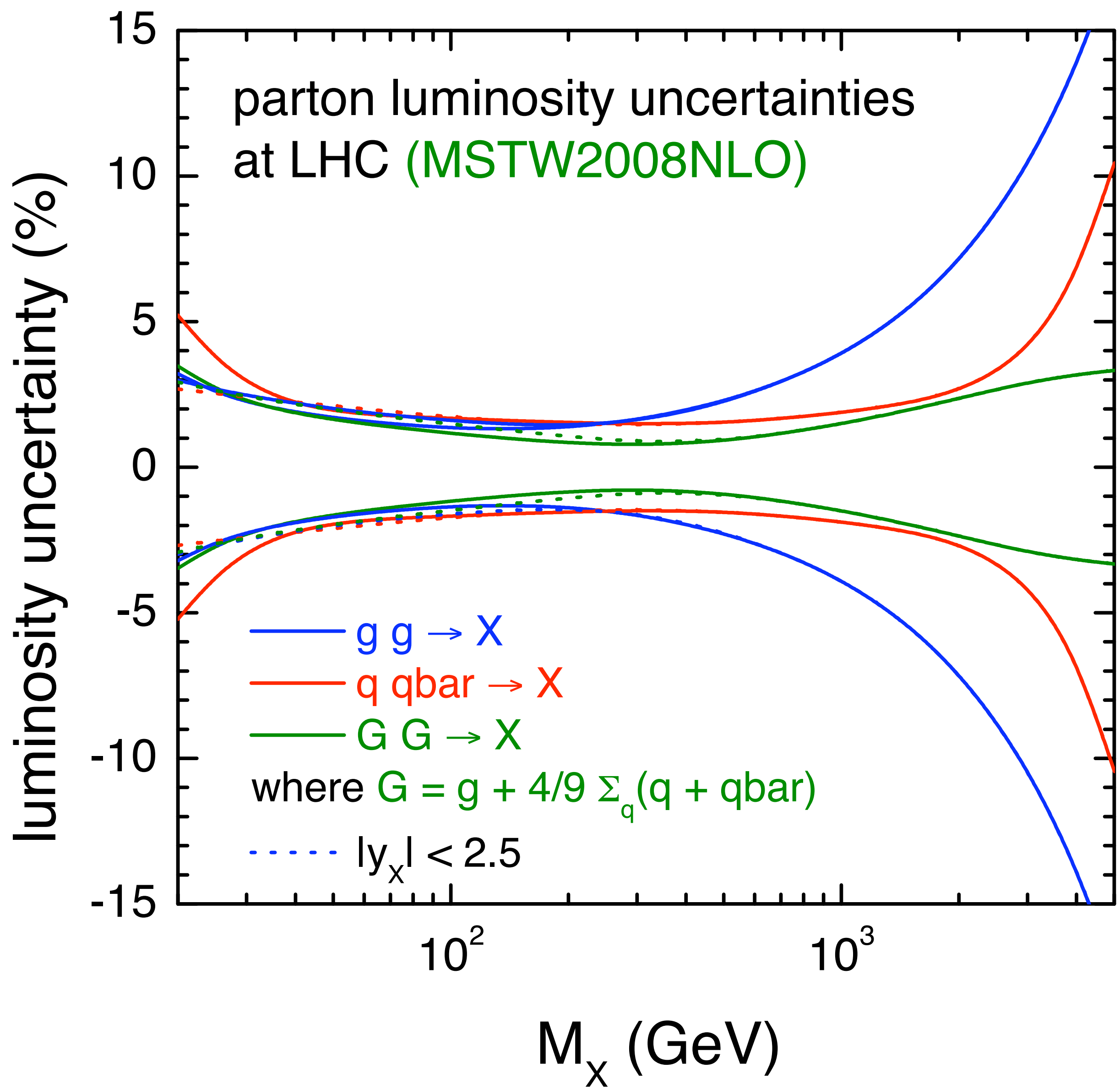

Conclusions

Have new MSTW2008 PDF sets at LO, NLO and NNLO, all with uncertainties.

Various changes in method of determining uncertainties.

Inclusion of a lot of new data. Dimuon data fitted directly. Important constraint on strange. New uncertainties on $s + \bar{s}$ feed into other partons.

Allows increase in number of parameters (and better choice of parameters) in eigenvector determination. Hessian approach improves as more data constraint allows more free parameters. Perhaps now underestimate at very high ($\geq 0.6 - 0.7$) x and for $x \ll 0.01$ for valence quarks, or flavour dependent combinations.

New algorithm for tolerance for uncertainties. No fixed $\Delta\chi^2$, but scan over each eigenvector direction and using confidence level criterion.

On average $\Delta\chi^2 \sim 40$ for 90% confidence limit $\Delta\chi^2 \sim 16$ for $1 - \sigma$. Should, in principle, be conservative.

Fully include uncertainty from normalization effects. Additional normalization uncertainty $\sim 1\%$.

Note that MSTW2008 and NNPDF sets sometimes differ significantly in central values though.

Clearly seen for up valence and anti-up distributions.

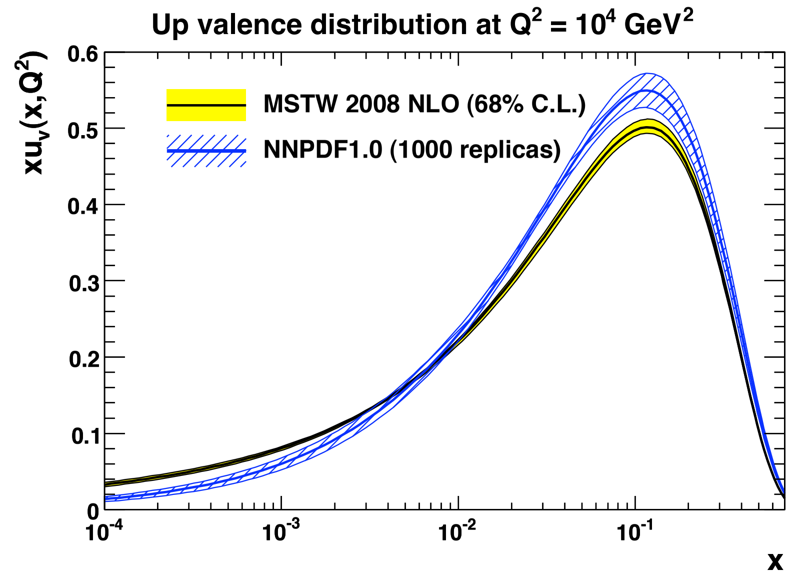

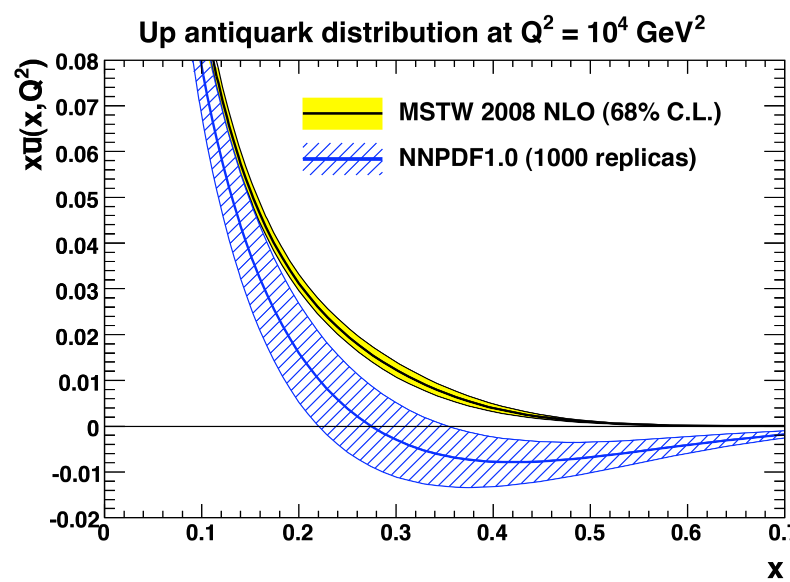

Strange itself has some non-insignificant mass, and this should qualitatively lead to suppression compared to light sea quarks up and down.

When c and b turn on they evolve like massless quarks, but always lag behind. $\rightarrow$ some suppression at all x for finite Q^2.

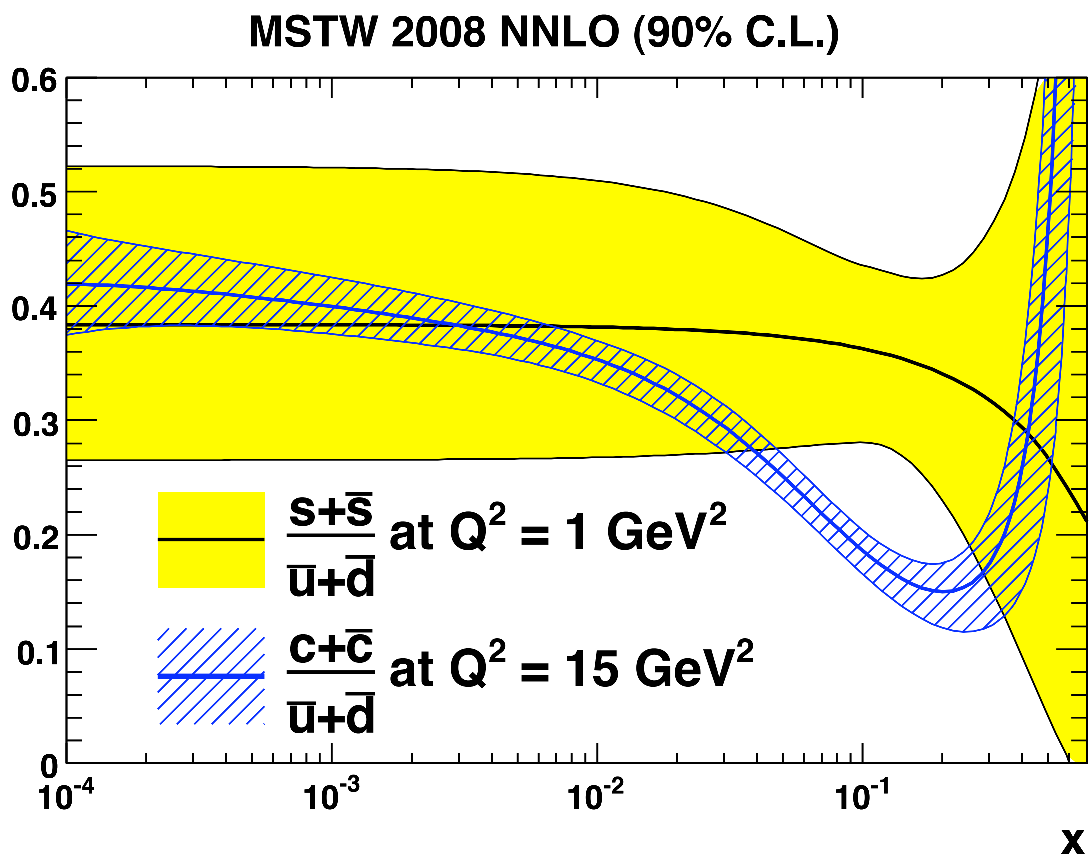

$c + \bar{c}$ evolved through $\sim 7 - 8$ times input scale similar to $s + \bar{s}$ at $Q^2 = 1\mathrm{GeV}^2$. Do not expect exact correspondence, but very good except $c + \bar{c}$ more suppressed at $x \sim 0.1$. (Implication for $s + \bar{s}$ from recent HERMES $K^{\pm}$ data).

Initial Running

Of course, will be starting the LHC running at 10 TeV rather than the full 14 TeV.

Roughly $60-70\%$ the full cross-sections for most standard model (including light Higgs) processes.

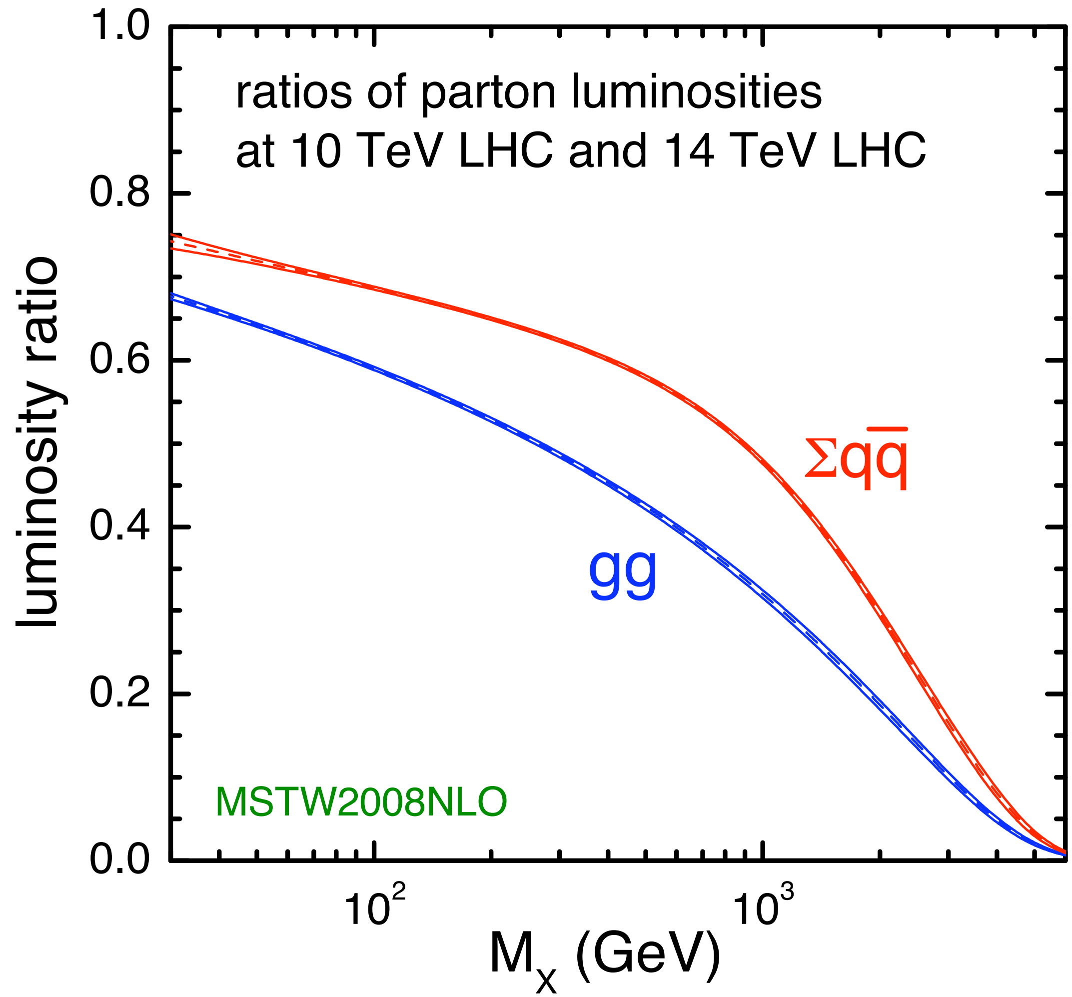

Predictions – Cross-sections

Predictions for W and Z cross-sections for Tevatron with common fixed order QCD and vector boson width effects, and common branching ratios.

Fairly significant change from NLO to NNLO mainly due to hard cross-section correction.

Other than this reasonable agreement in predictions.

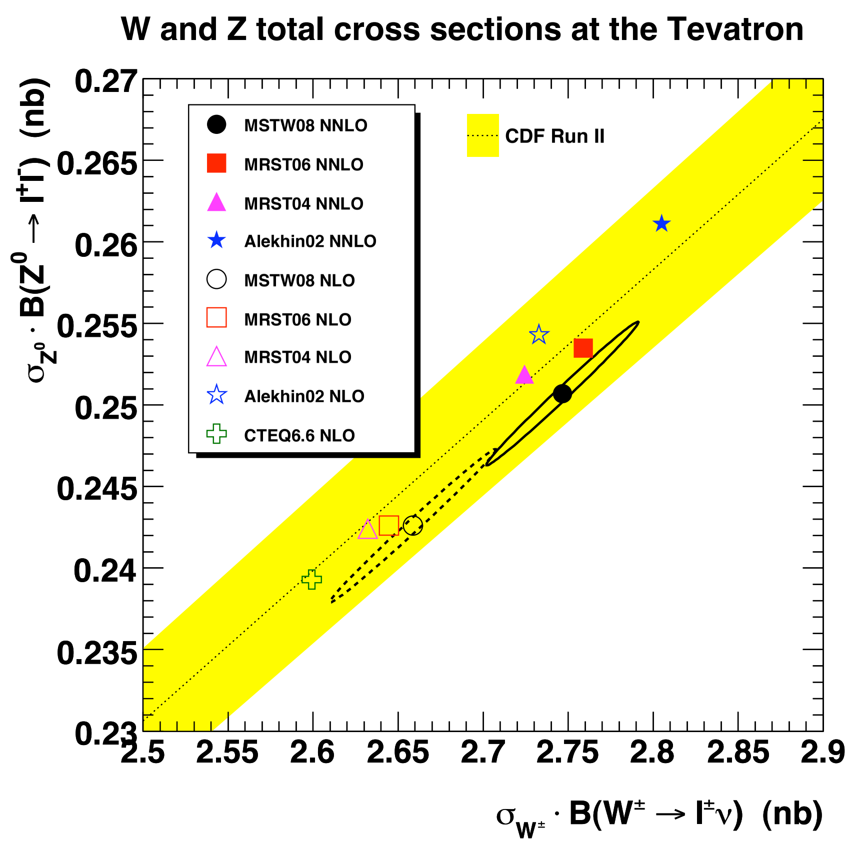

Predictions for W and Z cross-sections for Tevatron with common fixed order QCD and vector boson width effects, and common branching ratios.

Increases from MRST2006 compared to MRST2004 due to changes due to improved (NLO) or completed (NNLO) heavy flavour prescription.

Virtually no change from MRST2006 $\rightarrow$ MRST2008. Ratio changes due to change in strange distribution.

Reasonable agreement at NLO with CTEQ6.6, but systematic difference mirrors shape of gluon/quarks.

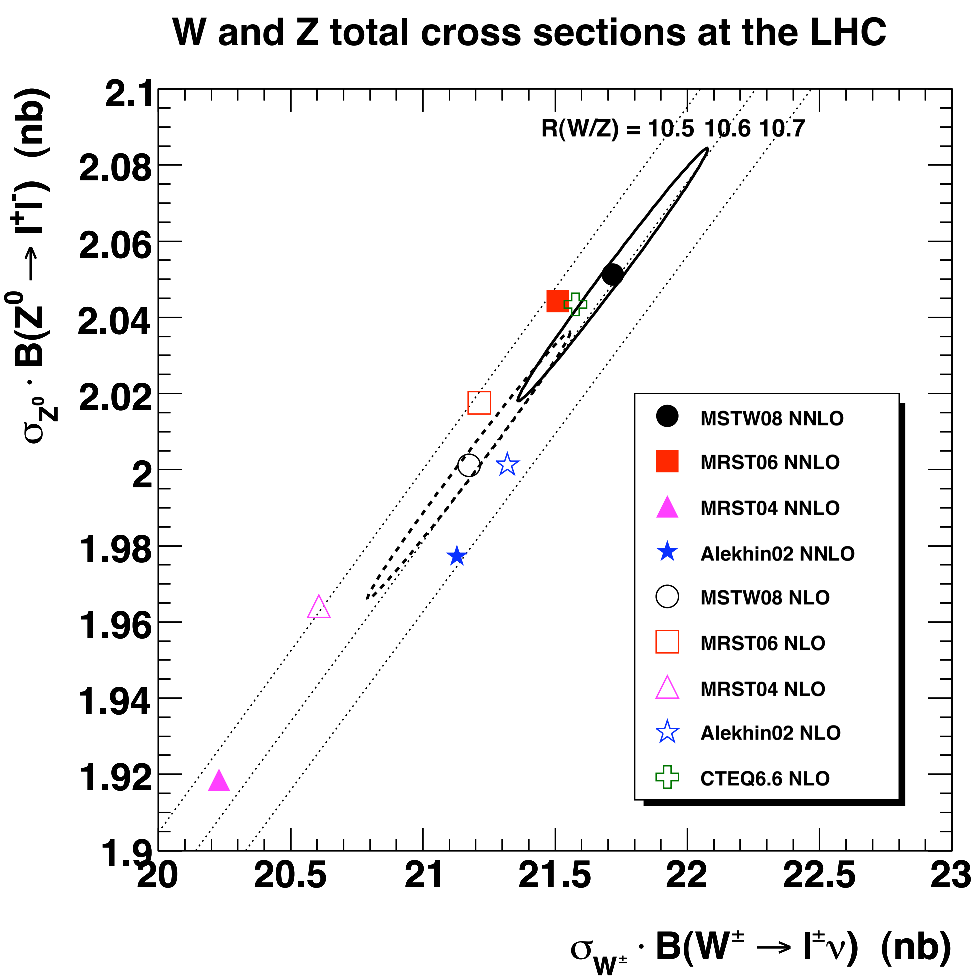

Uncertainty – more details

Uncertainty on $\sigma(Z)$ and $\sigma(W^+)$ grows at high rapidity.

Uncertainty on $\sigma(W^-)$ grows more quickly at very high y – depends on less well-known down quark.

Uncertainty on $\sigma(\gamma^\star)$ is greatest as y increases. Depends on partons at very small x.

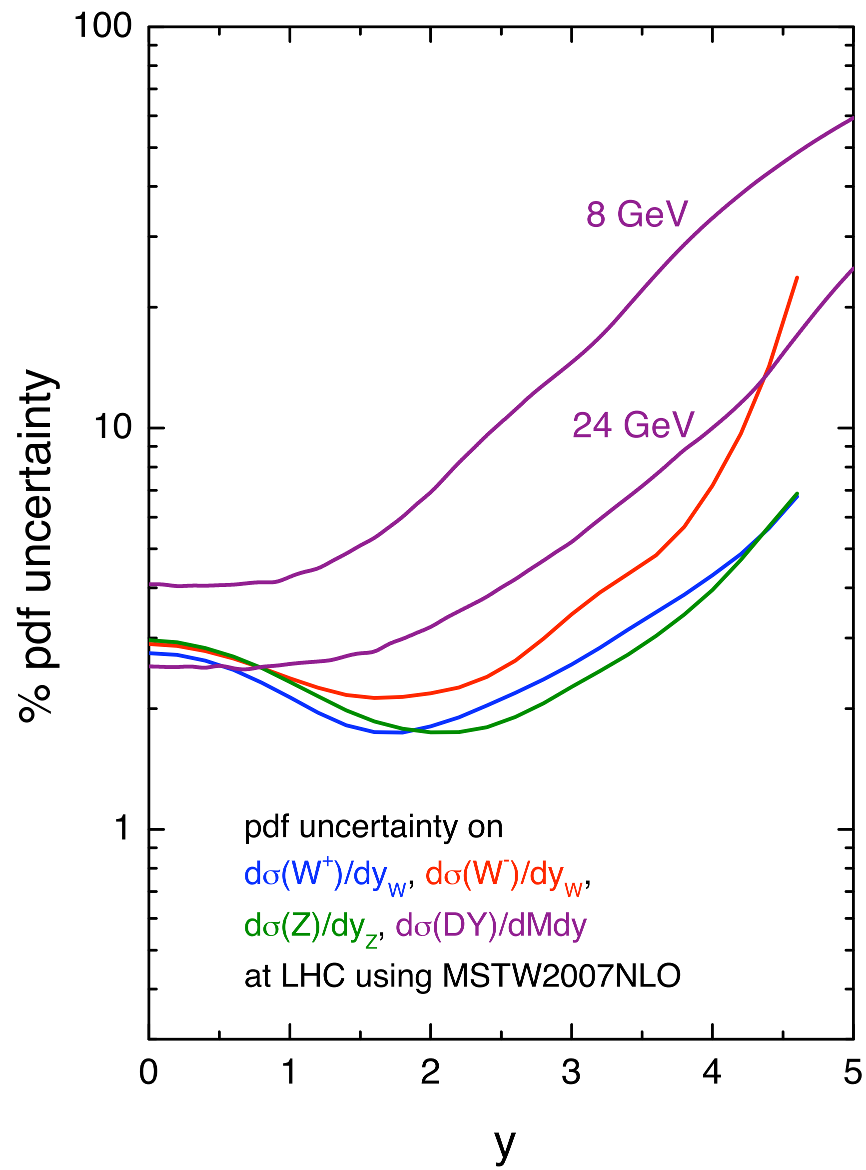

More information from ratios including $\sigma(Z)$, $\sigma(W^-)$ and $\sigma(W^+)$.

Cleaner experimentally.

Uncertainty on A_W large even just from experimental sources.

But $y = 0$ is $x_1 = x_2 = 0.006$ – range of extrapolation of valence quarks. Differences in different PDF extractions.

One of most useful inputs to PDFS with very little data.

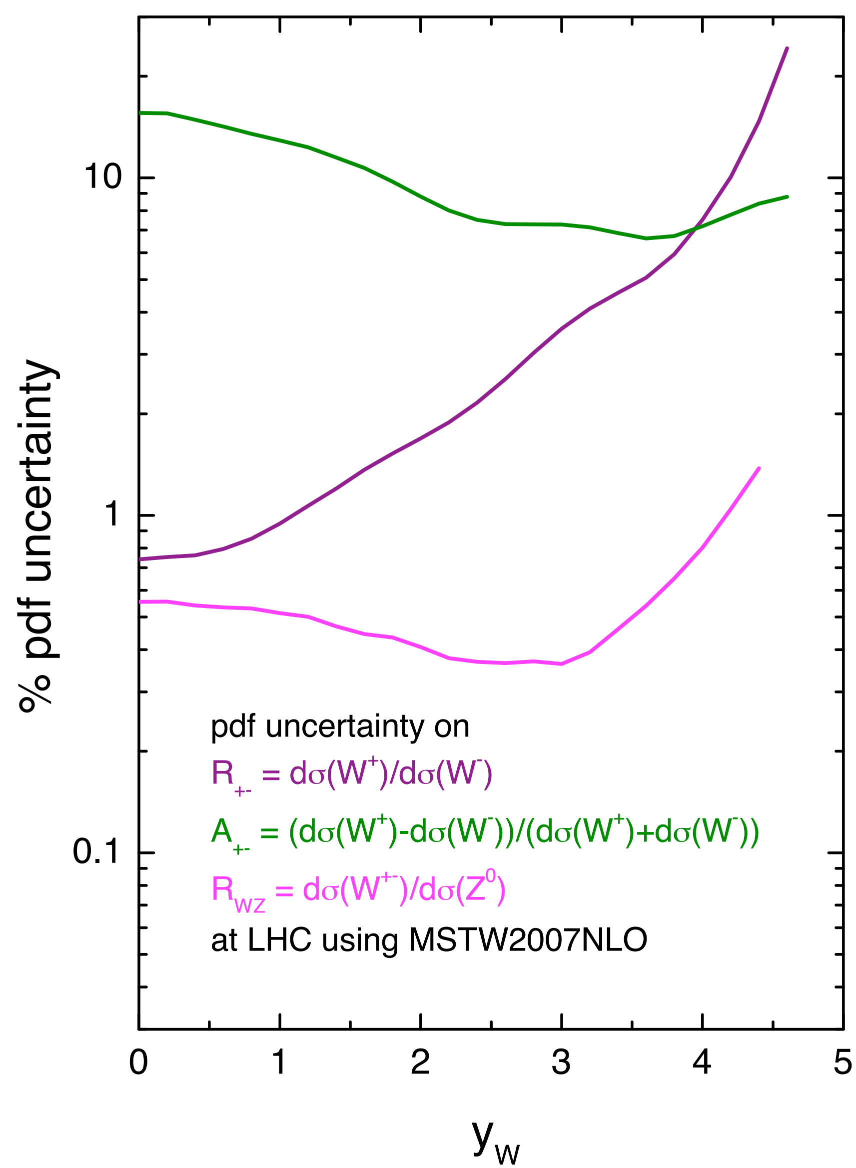

Extremely small uncertainty on ratios W/Z and W^+/W^-.

Predictions for W+ and W- cross-sections for LHC with common fixed order QCD and vector boson width effects, and common branching ratios.

Quoted uncertainty for ratio very small, i.e. $\approx 0.8\%$.

Significantly more difference in this from other PDFs, including MRST.

Again very interesting for early data.

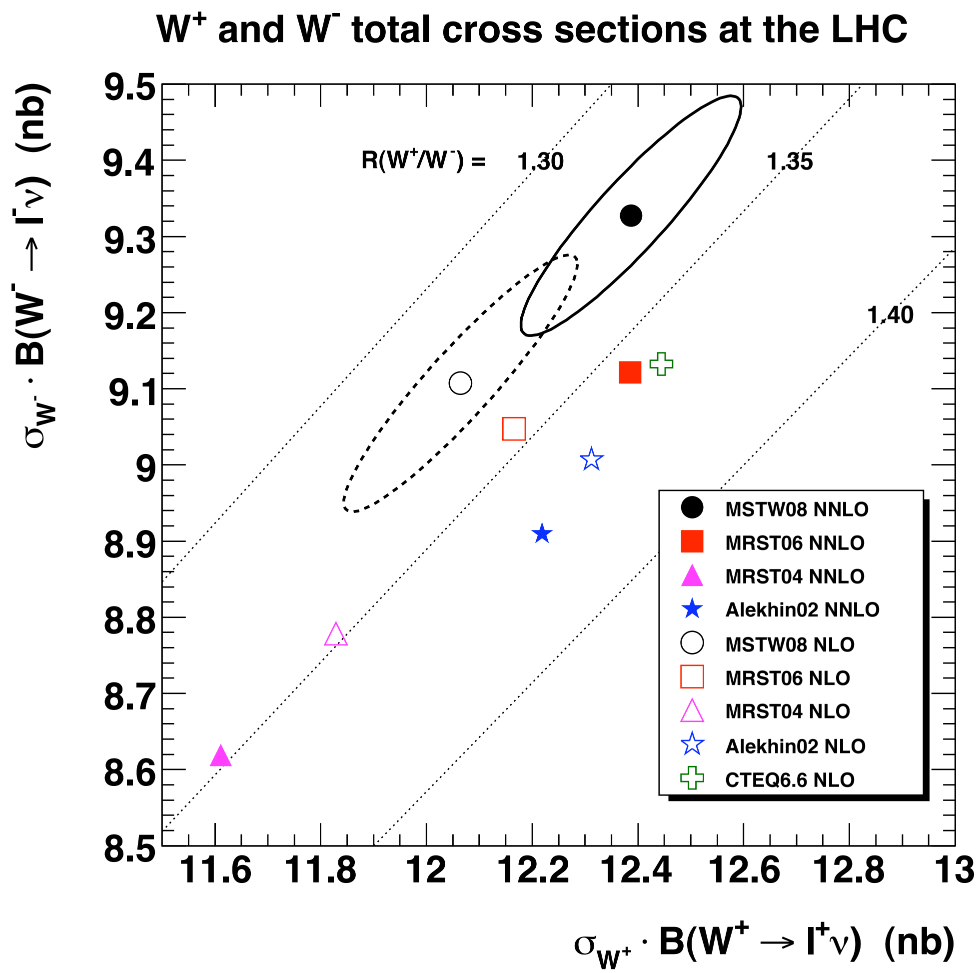

Perturbative Stability at the LHC

Now have QCD calculations at LO, NLO and NNLO in the coupling constant α_S for Z, W and $\gamma^\star$ production Anastasiou, Dixon, Melnikov, Petriello).

Good stability in predictions for e.g. Z and $\gamma^\star$ cross-sections for very high virtuality.

Becomes worse at lower scales where α_S larger and large $\ln(s/M^2)$ terms appear in expansion (equivalent to $\ln(1/x)$) and large threshold $\ln(1-x)$ terms.